

4. OXIDATION BEHAVIOR AND EMBRITTLEMENT THRESHOLD OF THE MODIFIED E110 CLADDING: PROGRAM AND DISCUSSION OF TEST RESULTS

4.1. *Major provisions of the test program with a modified E110 cladding*

The results of the test program performed with the E110 standard as-received tubes and presented in chapter 1 of the report have shown that:

- the zero ductility threshold of the E110 alloy is lower than that of the Zry-4 alloy;
- the earlier initiation of the breakaway oxidation accompanied by hydrogen absorption in the prior β -phase of the E110 cladding is the major reason for the different mechanical behavior of oxidized claddings fabricated of these two alloys.

The numerous sensitivity studies performed in the frame of this work allowed to establish that variations in oxidation modes may somewhat hasten or delay the initiation of the breakaway oxidation in the E110 alloy, however, any variations in test conditions do not allow to avoid completely this type of oxidation in the ECR range of interest.

Approximately the same conclusion was made basing on the analysis of results of tests performed to check the correlation between some alloying elements (O, Fe, Sn) and the oxidation behavior of niobium-containing claddings.

All these results allowed to report the following general question: is this oxidation behavior typical of the whole family of niobium-bearing alloys or only of the E110 alloy? The comparison of the E110 test results with the published data on the other Zr-1%Nb alloy, namely, the M5 alloy [1, 2], allowed to reveal the following:

- the M5 and Zry-4 claddings are characterized by the similar embrittlement threshold at 1100 C;
- the breakaway oxidation was not observed on the M5 claddings in the tested ECR range.

A careful analysis of the existing situation allowed to assume that the specific behavior of the E110 cladding may be the consequence of two groups of effects connected with the cladding fabrication:

1. Surface effects.
2. Bulk effects.

The surface effects combine such factors as the surface chemistry (surface contaminations) and surface roughness. In their turn, bulk effects may be the manifestation of such factors as the cladding material chemical composition (the composition of impurities) and microstructure effects (the phase composition, grain size, parameters of the secondary precipitates, etc.).

As for the surface effects, it is known that the surface finishing of cladding tubes is the important component for the cladding corrosion resistance. Thus, for illustration, the results of this work confirm the numerous observations concerning the relationship between the initiation of the breakaway oxidation and the localization of the cladding surface scratches (see Fig. 4.1).

To provide the chemical cleaning and chemical polishing of the E110 cladding tube, the standard procedure for the E110 surface finishing is used. This procedure includes the chemical etching and anodizing of the outer surface of the E110 fuel rod. Besides, special studies are performed at present to develop the modified method for the E110 surface finishing. One of the potential variants of new approaches to this problem is the grinding of the cladding outer surface and the jet etching of the cladding inner surface. Taking into account all these considerations, it was decided to perform several special tests to assess the sensitivity of the E110 oxidation behavior to surface effects.

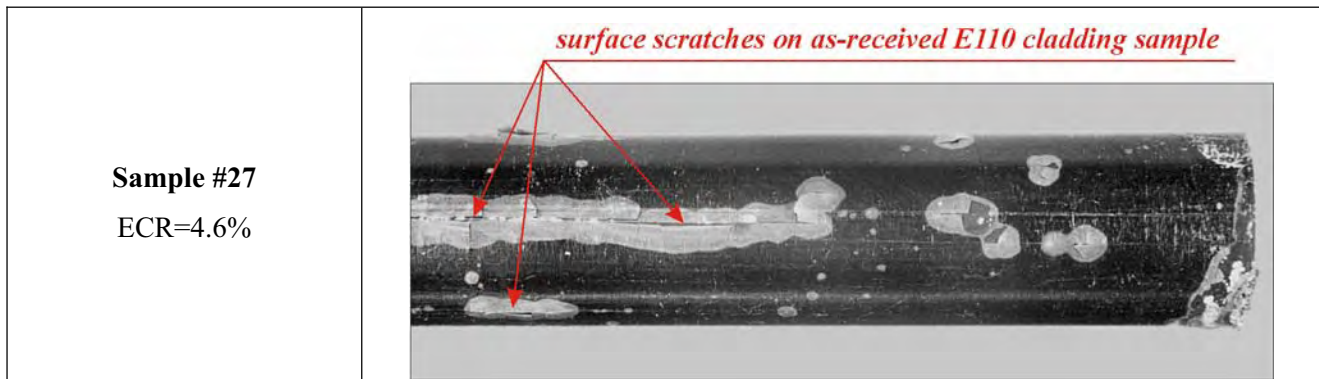


Fig. 4.1. The relationship between surface scratches and localization of the breakaway oxidation areas

The studies of bulk effects associated with the oxidation behavior of niobium-bearing alloys were the subject of numerous investigations performed in Russia and other countries. As for the microstructure effects, the analysis of publications allowed to note the following:

- the corrosion properties of binary zirconium-niobium alloys depend directly on the content and phases of the zirconium and niobium [3];
- the formation of equilibrium α -Zr and β -Nb phases leads to the improvement of corrosion resistance of binary alloys [3];
- the corrosion properties of the E110 alloy depend on the material microstructure; the annealing temperature and duration are the major factors determining the cladding microstructure; the annealing at 580 C during 3 hours (below the monoeutectoid line) leads to the maximum depletion of the α -Zr matrix by the niobium and to the formation of the β -Nb phase that improves the alloy corrosion resistance [4];
- the corrosion behavior of the E110 alloy cladding is shown to be strongly dependent on the material structure (including the grain size), the formation of the completely recrystallized material with a fine grain size determines the best corrosion resistance [5];
- a strong dependence of corrosion properties of binary alloys on heat treatment was revealed; the formation of metastable phases at the annealing temperature higher than the monoeutectoid one leads to the very low corrosion resistance, the annealing in the temperature range of the α -Zr phase presence leads to the formation of the equilibrium structure and high corrosion resistance [6];
- to prevent the degradation in the corrosion resistance, the intermediate and final annealing temperature must not exceed 600 C; in this case, the material of M5 tubes remains in the α -Zr plus β -Nb region under completely recrystallized conditions [7];
- the samples of Zr-xNb binary alloys annealed at 570 C to form β -Nb phase showed a much lower corrosion rate and higher volume fraction of tetragonal ZrO_2 in the oxide than those annealed at 640 C to form β -Zr phase [8];
- basing on the consideration of publications devoted to the corrosion behavior of niobium-bearing alloys, the authors of investigations presented in [9] have declared that the correlation between the oxide characteristics and microstructure or microchemistry, such as β phases, Nb-containing precipitates and soluble Nb in the matrix, is not well understood in Zr-Nb alloys. One of the major results of investigations performed by these researchers could be formulated as following: at high Nb-contents 1.0–5.0 wt%, the corrosion rate was very sensitive to the annealing condition, the transformation of the oxide structure from tetragonal ZrO_2 to monoclinic ZrO_2 and of the oxide microstructure from the columnar to equiaxed structure was accelerated in the samples having β -Zr phase. The corrosion rate of samples annealed at 570 C with the formation of the β -Nb phase was much lower. Moreover, it is assumed that the equilibrium concentration of Nb in the α -matrix would be a more dominant factor to enhance the corrosion resistance than the Nb-containing precipitates.

The above listed results of previous investigations have shown that the corrosion behavior of binary Zr-Nb alloys is very sensitive to the microstructure characteristics that in their turn are determined by the

fabrication procedures and conditions. In this case, the fact cannot be excluded that the annealing condition may be not the only key factor in spite of the fact that recent special studies performed with the M5 alloy have demonstrated that the corrosion resistance is not sensitive to many aspects of the fabrication process [7]. Unfortunately, a direct comparison of manufacturing procedures used on the fabrication of the E110 cladding and M5 cladding to reveal the differences that may be responsible for differences in the corrosion behavior of these two niobium-bearing claddings is not possible because this is confidential commercial information. Therefore, to provide the comparative analysis of possible microstructure effects in these two alloys, it was decided to perform a careful SEM (scanning electron microscopy) and TEM (transmission electron microscopy) examinations of the E110 cladding material and after that to compare the obtained results with the published data characterizing the M5 tube microstructure.

The next position of special investigations performed with the E110 cladding to study of bulk effects was devoted to the studies of the microchemical effects of the cladding material in the context of the E110 oxidation behavior. The analysis of results of previous investigations performed in this line allowed to reveal the following:

- the optimization of Nb concentration in the E110 alloy allowed to minimize the influence of N, Al, C impurities causing the degradation of the corrosion resistance [4];
- the secondary phase particles influence significantly the corrosion behavior of niobium-bearing alloys. Special investigations performed with the cladding samples the surface of which was modified due to the ion alloying have shown that a strong dependence is between the oxide structure and secondary intermetallic participates on the cladding surface. So, the oxide layer has a thickening in this area consisting of metal oxides of the secondary phase participates. The decrease of the participate density at the alloying process leads to the improvement of the oxide contact with the metal matrix [10];
- the corrosion tests have demonstrated that the alloying of the E110 cladding of such elements as Fe, Mo, Sn leads to the decrease in the oxidation rate [11];
- the presence of such elements as Sn, Fe, Cr, Nb improves the corrosion resistance of zirconium [6].

It is evident that the above listed results of previous investigations are remarkable for the fragmentariness and are insufficient to analyze microchemical bulk effects as applied to the corrosion behavior of the E110 alloys. The additional analysis of published data devoted to the relationship between the corrosion behavior of other zirconium alloys and their microchemical compositions has shown that in spite of a great number of investigations performed recently, a clear physical understanding of appropriate phenomena has not been achieved yet. Taking into account this circumstance, the further development of this line of investigations was based on the following considerations:

- if the microchemistry of Zr-Nb alloys is the key factor resulting in differences in the behavior of such two Zr-1%Nb alloys as E110 and M5, then this means that these two alloys have different compositions of impurities in the cladding material. In this case, this conclusion does not concern the differences in the oxygen concentration as this effect has been specially investigated (see chapter 1);
- the analysis of possible reasons for potential differences in the impurity composition and content of these two alloys has shown that two different methods are employed to fabricate the Zr-1%Nb ingot:
 - the sponge Zr is used on the manufacturing of the M5 cladding;
 - the mixture of iodide and electrolytic Zr is used on the manufacturing of the E110 cladding;
- the comparative description of these methods for the preparation of the Zr-1%Nb ingot is given in [12].

It should be noted that the Russian industry is planning in the nearest time to proceed to the employment of sponge Zr to manufacture the E110 cladding taking into account the economic advantage (the fabrication of iodide/electrolytic Zr is significantly more expensive than the fabrication of sponge Zr). In the frame of this work, different types of the E110 claddings were manufactured with the use of sponge Zr. Therefore, it was decided to perform the investigations of microchemistry effects associated with the oxidation behavior of the E110 alloy using several different types of the E110 cladding manufactured on the basis of sponge Zr.

In accordance with the above listed surface and bulk effects, the program of this stage of research was developed. The major provisions of this program are presented in Table 4.1.

Table 4.1. The E110 surface and bulk effects studies: major provisions of experimental program

Program stage	Major tasks	Comments
1. Surface effects investigations 1.1. Tests of the E110 etched and anodized cladding	To perform several oxidation tests with the E110 etched and anodizing cladding and to compare the mechanical behavior of the E110 cladding and E110 as-received tube	The commercial E110 etched and anodizing cladding should be used for these tests
1.2. Tests of the E110 cladding with the modified surface finishing	To perform oxidation tests with two types of surface finishing: 1. Grinding of the cladding outer surface and jet etching of the cladding inner surface 2. Polishing of the cladding outer and inner surfaces	The commercial advanced E110 cladding should be used for the first type of tests. The laboratory procedure for the preparation of special samples with polished outer and inner surfaces of the E110 as-received tubes should be used for the second type of tests
2. Bulk effect investigations: 2.1. Studies of the E110 cladding microstructure	To perform the SEM and TEM examinations of different types of the E110 claddings and to perform the comparative analysis of obtained microstructure characteristics	The samples of the E110 cladding material fabricated with the application of different methods for manufacturing of Zr-1%Nb ingot should be prepared for these examinations
2.2. Studies of dependence of the oxidation and mechanical behavior of the E110 cladding on the chemical composition of Zr-1%Nb	To perform oxidation tests with several types of the E110 and E635 as-received tubes fabricated with the use of sponge Zr-1%Nb. To compare the mechanical behavior of these claddings with the behavior of standard E110 tubes manufactured with the use of iodide/electrolytic Zr	Special cladding samples fabricated in accordance with the standard procedure but with the application of sponge Zr should be used for these tests

All oxidation and mechanical tests performed in the frame of this program were made in accordance with the following technical requirements:

- the oxidation type: the double-sided oxidation with the F/F combination of heating and cooling rates;
- the oxidation temperature: 900–1200 C;
- the characterization of mechanical tests: ring compression tests of 8 mm rings at 20 and 135 C.

4.2. The analysis of experimental results obtained at surface effect studies

As it was noted in section 4.1, three types of cladding samples were used to investigate these effects:

1. Standard E110 etched and anodized cladding (E110A).
2. E110 as-received tube with the modified surface finishing (the outer surface grinding and inner surface jet etching) performed at the tube plant (E110_m).
3. E110 as-received tube sample, one half of which remained in the initial state and the second half was polished from the inside and outside in the RIAR laboratory (E110_{pol}).

The whole scope of obtained test results is presented in Tables B-1 and B-2 of Appendix B. The appearances of the E110A and E110_m samples before and after oxidation tests are shown in Fig. 4.2.

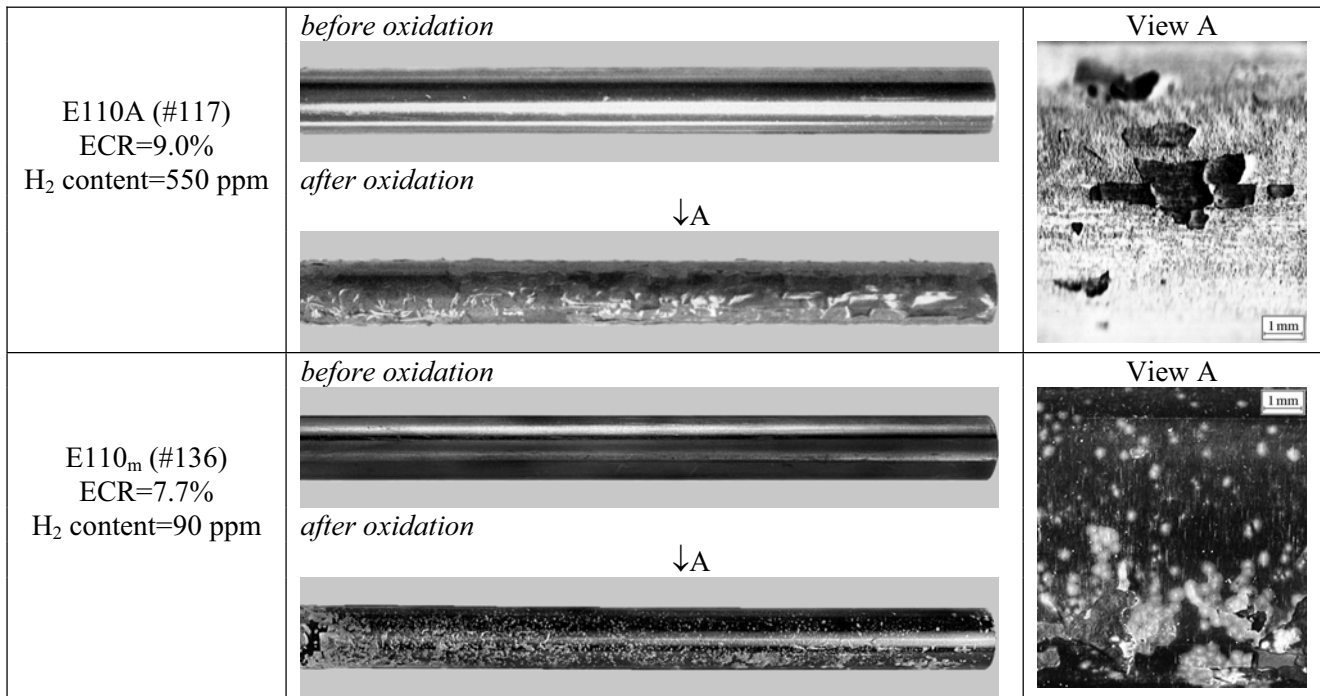


Fig. 4.2. The appearance of the E110 claddings fabricated with the use of two different types of surface finishing before and after oxidation tests at 1100 C

The analysis of these data allows to note the following:

- the standard surface finishing of the E110 cladding does not lead to improvements in comparison with the oxidation behavior of the E110 as-received tubes; the classic breakaway effect accompanied by the hydrogen pickup was observed on the cladding outer surface (see Fig. 4.3 also);
- the modified surface finishing of the E110 tube on the basis of the outer surface grinding and inner surface jet etching does not allow to eliminate the breakaway oxidation. The oxidized cladding appearance and the microstructure of oxides formed on the inner and outer cladding surfaces (see Fig. 4.3) show that the spallation and delamination of ZrO₂ oxide are observed on both surfaces of the cladding. Moreover, the oxide thickness on the etched inner surface is larger than that on the grinded outer surface.

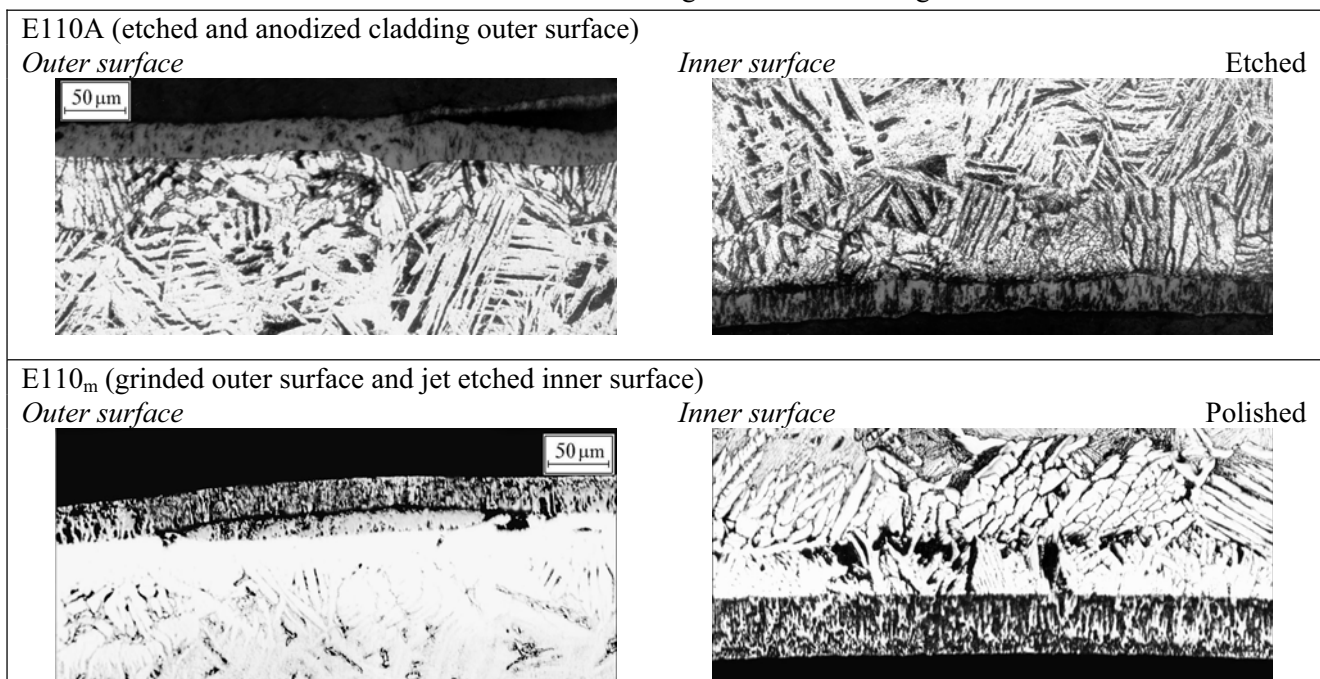


Fig. 4.3. The microstructure of the E110A and E110_m claddings after the oxidation at 1100 C

Obtained observations are in the reasonable agreement with results of ring compression tests performed with the 8 mm samples cut off from 100 mm oxidized samples (see Fig. 4.4). Moreover, numerous special investigations performed in the ANL with the E110 samples which underwent different procedures of the cladding etching and the cladding cleaning after etching have demonstrated that etching is more than undesirable procedure from the point of view of the E110 cladding oxidation behavior [13]. This conclusion is confirmed by the results of previous studies of zirconium alloys [14]. Taking into account a very high sensitivity of the breakaway initiation to the minimum presence of F-contamination on the cladding surface (that was demonstrated many times in previous investigations), it may be assumed that fluorine containing particles remain on the etched cladding surface, though this assumption contradicts the results of the appropriated check procedures that are performed at tube plant. Unfortunately, it was impossible to perform special measurements of fluorine contents on the cladding surface in the frame of this work as those are very difficult from the methodological point of view.

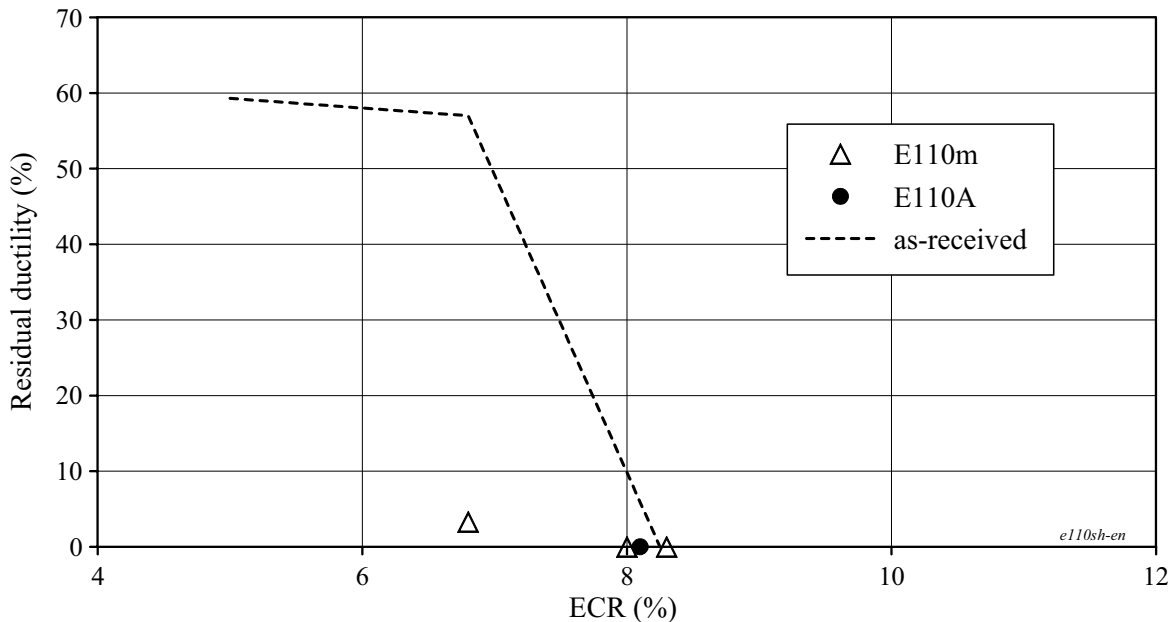


Fig. 4.4. The comparison of residual ductility of the standard E110 as-received tube, E110A and E110_m claddings after the oxidation at 1100 C

The indirect confirmation of this reason for the E110 breakaway initiation was obtained from the results of investigations performed in the ANL. They performed additional polishing of the outer and inner surfaces of the E110A cladding. In this case, the cladding inner diameter was increased after polishing by 100 μm. The oxidation tests at 1100 C and ring compression tests have shown that the margin of residual ductility remains in these claddings up to 16% ECR (as-measured) [13].

The similar tests were performed in the frame of this work also. Polishing of one half of the E110 sample 100 mm long was performed on the inner and outer surfaces of the E110 as-received tube. The second half of this sample remained intact. The surface roughness on the polished part of the cladding sample was about 0.08–0.16 μm that corresponds to the surface roughness of the M5 and Zry-4 claddings (0.1–0.15 μm). Taking into account the effect of the oxidation temperature revealed during the first part of research program, the oxidation tests of these samples were carried out at 1000 and 1100 C. The organized tests are presented in Fig. 4.5. The tabular results of tests are listed in Tables B-1 and B-2 of Appendix B.

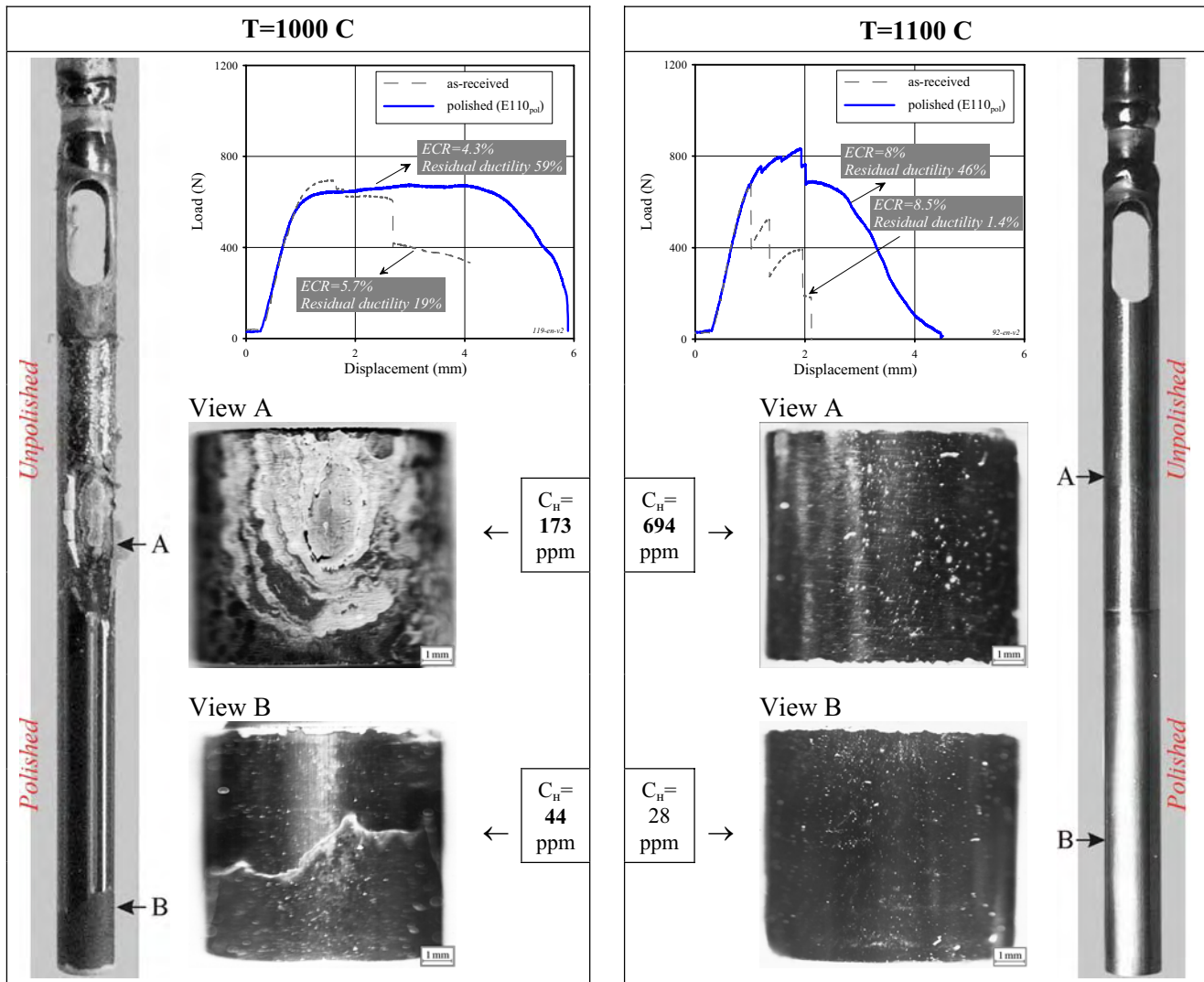


Fig. 4.5. Demonstration of sensitivity of the oxidation and mechanical behavior for the E110 cladding to the cladding surface polishing

The analysis of obtained comparative data allowed to reveal the following important aspects of the E110 oxidation behavior as a function of the cladding surface machining:

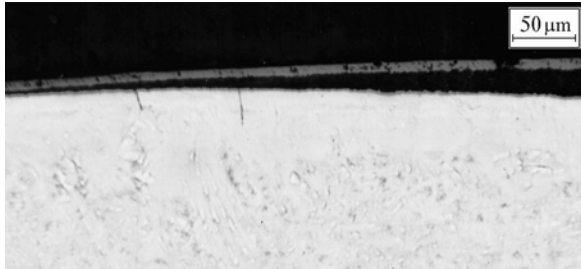
- the rate of the E110 cladding unpolished part oxidation is higher than that of the polished region;
- indications of the breakaway oxidation including the hydrogen absorption practically disappear on the polished part of the E110 cladding. This process takes place especially clearly on the oxidation at 1000 C;
- the residual ductility of the E110 cladding polished part is many times increased in comparison with the oxidized cladding unpolished part.

The additional information to characterize the appropriate cladding behavior may be obtained due to the consideration of the oxidized cladding microstructure in the polished and unpolished parts (see Fig. 4.6). As can be observed, the oxide spallation is noted on the outer surface of cladding unpolished part. The contact of oxide with the cladding matrix on the inner side is somewhat better but it is seen that a systematical layer of pores has been already generated on the interface between the oxide and metallic matrix, and, consequently, the oxide layer spallation will take place at the ECR increase. Another case is observed on the oxidized cladding polished part. The uniform oxide layer having a good adhesion with the metallic matrix covers the cladding outer and inner surfaces. This oxide behavior provides the lower oxidation rate and low rate of hydrogen diffusion into the E110 cladding.

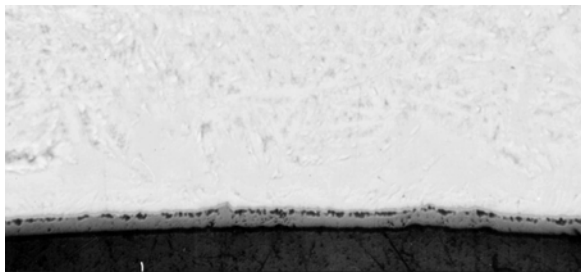
#119

Unpolished part

Polished



Polished

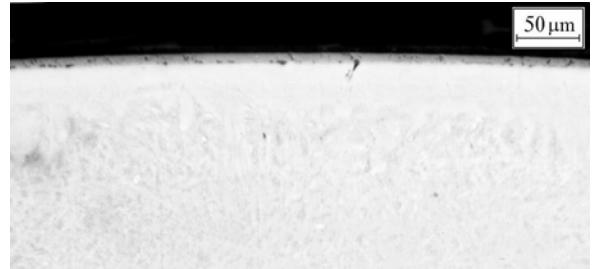


Etched

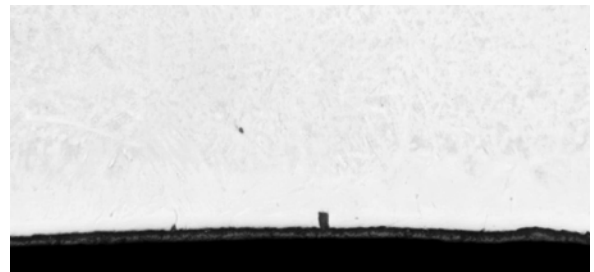


Polished part

Polished



Polished



Etched

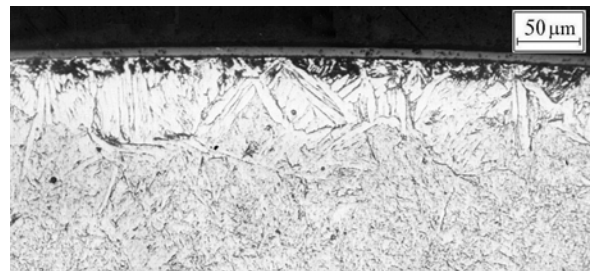


Fig. 4.6. The oxide microstructure on the polished and unpolished parts of the E110 cladding after the oxidation at 1000 C

The same results were obtained from the tests with polished E110 claddings in the ANL [13]. Polishing of the E110 cladding surface allowed to delay greatly the breakaway initiation, that in its turn resulted in the significant improvement of the oxidized cladding mechanical properties.

The results of tests with polished E110 claddings do not allow to formulate the final conclusion concerning the mechanism due to which the E110 cladding oxidation behavior is improved. However, turning back to the consideration of two possible reasons for the surface effect (the surface roughness and surface contamination) and taking into account the obtained test data, the following may be assumed:

- both factors are important for the initiation of the breakaway oxidation;
- but even an ideal surface state from the point of view of the surface roughness does not allow to avoid the breakaway oxidation at the low ECRs in the presence of the surface contaminations that is confirmed by the tests with etched claddings.

Thus, the microchemistry of the cladding surface is apparently the dominant factor influencing the break-away condition. The further analysis of microchemical effects will be continued in the next section of the report.

4.3. *The assessment of relationship between the microchemical composition and oxidation behavior of niobium-bearing alloys*

To study these potential effects of the cladding behavior, several types of zirconium niobium claddings were selected for the oxidation and mechanical tests. The specification for the used cladding material is presented in Table 4.2. The additional information characterizing the cladding initial parameters is given in Tables A-1, A-2 of Appendix A.

Table 4.2. The specification for the used cladding material

Notation conventions of cladding types used in this program	Alloying composition	Input components used on the fabrication of the alloy ingot
E110	Zr-1%Nb	Iodide Zr, electrolytic Zr, recycled scrap, Nb
E110 _{G(fr)}	Zr-1%Nb	French sponge Zr (CEZUS), Nb
E110 _{G(3fr)}	Zr-1%Nb	French sponge Zr, iodide Zr, recycled scrap, Nb
E110 _{G(3ru)}	Zr-1%Nb	Russian sponge Zr, iodide Zr, recycled scrap, Nb
E110 _{low Hf}	Zr-1%Nb	Iodide Zr, electrolytic Zr with low Hf content, recycled scrap, Nb
E635	Zr-1%Nb-1.2%Sn-0.35%Fe	Iodide Zr, electrolytic Zr, recycled scrap, Nb, Sn, Fe
E635 _{G(fr)}	Zr-1%Nb-1.2%Sn-0.35%Fe	French sponge Zr (CEZUS), Nb, Sn, Fe

All types of these claddings were manufactured in accordance with the Russian process for the cladding fabrication. The subprogram of experimental investigations with the cladding material manufactured with the use of sponge Zr and electrolytic Zr with low Hf contents consisted of positions listed in Table 4.3.

Table 4.3. The subprogram major tasks for the test with the sponge cladding material and E110 cladding with low Hf content

Task	Motivation
1. To perform the oxidation tests at 1100 C of the E110 and E635 claddings manufactured with the use of 100% sponge Zr (E110 _{G(fr)} , E635 _{G(fr)}) and to perform the ring compression tests of oxidized claddings	To develop the comparative test data on the behavior of iodide/electrolytic E110 and E635 alloys and sponge E110 and E635 alloys
2. To perform the tests with the E110 cladding manufactured by the standard Russian procedure but with low Hf content in the electrolytic Zr (E110 _{low Hf})	Taking into account that the chemical composition of the standard E110 cladding is characterized by a very high content of Hf (in comparison with the sponge material), to check the dependence of the E110 oxidation behavior on Hf content
3. To perform the oxidation tests at 1100 C of the E110 claddings manufactured from the mixture of iodide, sponge Zr and recycled scrap, after that to estimate the mechanical behavior of oxidized samples (E110 _{G(3ru)} , (3fr))	To clarify the sensitivity of the cladding oxidation behavior to the variation in the microchemical composition of the E110 alloy

Task	Motivation
4. To perform the oxidation tests at 900, 1000, 1200 C with the use of sponge types of the E110 cladding material and to estimate the margin of residual ductility of oxidized samples	To determine the representativity of test results obtained at 1100 C for other temperature regions

The whole scope of test results obtained in the frame of this subprogram is presented in Tables B-1, B-2 of Appendix B and in Appendix H of the report. The major outcomes of the subprogram are discussed in the next paragraphs of this section.

4.3.1. The analysis of the oxidation and mechanical behavior for the E110_{G(fr)} and E635_{G(fr)} claddings fabricated on the basis of 100% French sponge Zr

Two samples from this type of the E110 cladding were oxidized at 1100 C. The appearances of samples after the oxidation tests are presented in Fig. 4.7.

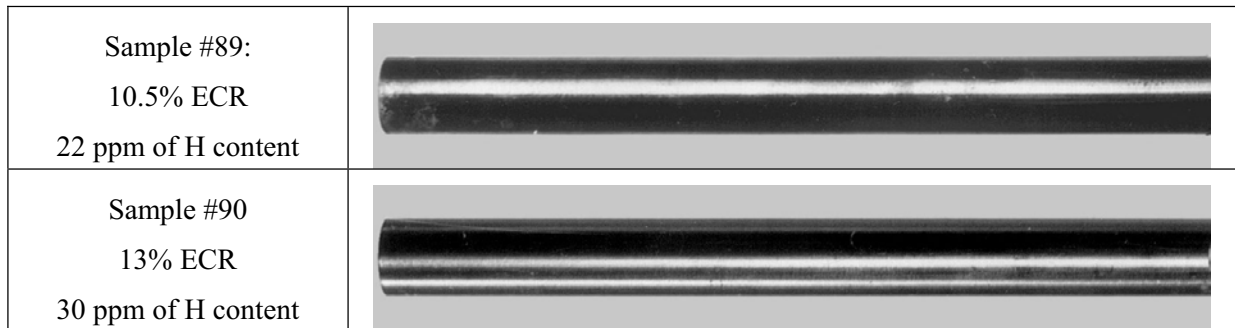


Fig. 4.7. Appearances of E110_{G(fr)} samples after the double-sided oxidation at 1100 C

The appearance of these samples demonstrates that in spite of a high level of measured ECRs (10.5 and 11.0%) the cladding surface is covered with the black bright oxide. This fact indicates that the mechanism of the uniform oxidation was realized on testing of these samples. The results in detail of mechanical tests with this type of the E110 cladding in comparison with the results obtained in the test with the standard E110 cladding allow to note the following (see Fig. 4.8):

- the E110_{G(fr)} oxidized rings have a visible residual plastic deformation after the ring compression tests;
- the load-displacement diagrams of the E110_{G(fr)} oxidized samples demonstrate that a significant part of the sample deformation before the fracture was accompanied by the plastic strain;
- both E110_{G(fr)} oxidized samples are characterized by a very low hydrogen concentration;
- the E110_{G(fr)} oxidized claddings have a significant margin of residual ductility at 13% ECR (as-measured); this margin corresponds to that for the Zry-4 cladding.

This first stage of appropriate investigations has shown that E110 claddings fabricated in accordance with the traditional Russian method of ingot preparation and E110 claddings fabricated in accordance with the western method of ingot preparation have quite a different oxidation behavior.

In the context of investigations presented in this section of the report, the revealed differences may come from the differences in the microchemical composition (impurity content) of the E110 and E110_{G(fr)} cladding materials. To extend the data base for the analysis of these effects, intermediate compositions of cladding materials such as E110_{G(3fr)} and E110_{G(3ru)} were tested.

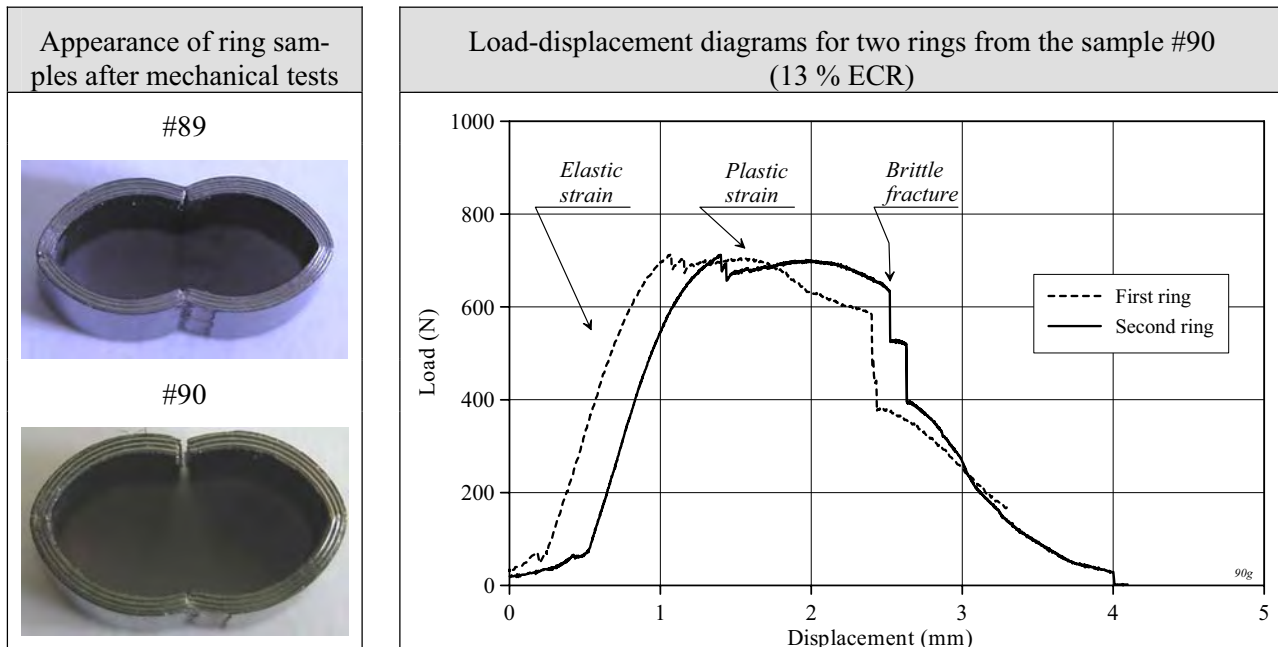


Fig. 4.8. Results of ring compression tests with E110_{G(fr)} oxidized samples

4.3.2. The interpretation of test results with E110_{G(3fr)} and E110_{G(3ru)} claddings

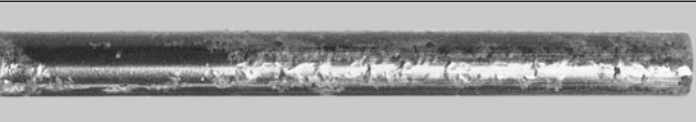
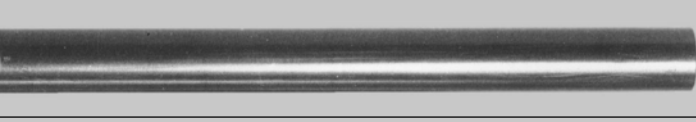
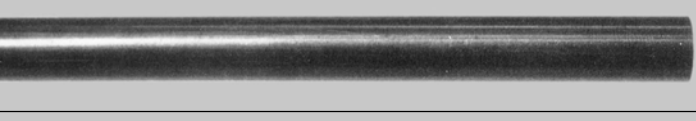
The appearances of these samples after the oxidation test in comparison with the standard E110 cladding and the results of mechanical tests are shown in Fig. 4.9 for an oxidation temperature of 1100 C.

The obtained data showed that all effects revealed in the analysis of the E110_{G(fr)} behavior (a black bright oxide, low hydrogen content, high margin of residual ductility up to 16.7% ECR), were confirmed in the tests of the E110_{G(3fr)} and E110_{G(3ru)} claddings. This observation indicates that in spite of the fact that E110_{G(3fr)} and E110_{G(3ru)} claddings contain only 70% of sponge Zr-1%Nb this turned out to be enough to improve considerably the oxidation behavior of the E110 cladding.

The additional confirmation of this conclusion can be obtained due to the comparative analysis of the cladding microstructures presented in Fig. 4.10. As can be seen from this data, the prior β -phase of the cladding samples manufactured from the iodide/electrolytic alloy and oxidized to the 10.0% ECR (#65) was so embrittled that local areas of the prior β -phase flaked off on polishing of the metallographic sample (black areas on the sample surface). Besides, this sample has no clearly marked boundary between the α -Zr(O) and prior β -phases. In contrast to this cladding, the cladding manufactured on the basis of sponge Zr (#89) is characterized by a clear boundary line between α -Zr(O) and prior β -phases and the structure of the prior β -phase without visible indications of α -Zr(O) phase and solid hydrides.

As a whole, these differences indicate that the diffusion processes in these two types of the E110 cladding determining the diffusion of alloying elements (including such minor alloying elements as impurities), proceeded in these cladding in different ways. It may be assumed that these differences represent the key factor predetermining the differences in the oxygen and hydrogen pick up and the distribution in the E110 standard and E110 sponge claddings. At this stage of the preliminary analysis of revealed effects the so-called “hafnium issue” arose.

The basis for the hafnium issue lies in the fact that hafnium concentration in the E110 standard alloy (up to 500 ppm) and hafnium concentration in the E110 alloy fabricated with the use of sponge (<100 ppm) differ greatly. Therefore, in spite of the fact that the difference in the Hf concentration cannot cause the general difference in the oxidation behavior of these cladding from the physical point of view, it was decided to perform special investigations to study this effect.

E110 (standard)	#96 9.8% ECR	
E110 _{G(3ru)}	#95 11.6% ECR (4 ppm of H content)	
E110 _{G(3fr)}	#99 11.5% ECR (13 ppm of H content)	
E110 _{G(3ru)}	#97 16.7% ECR (17 ppm of H content)	

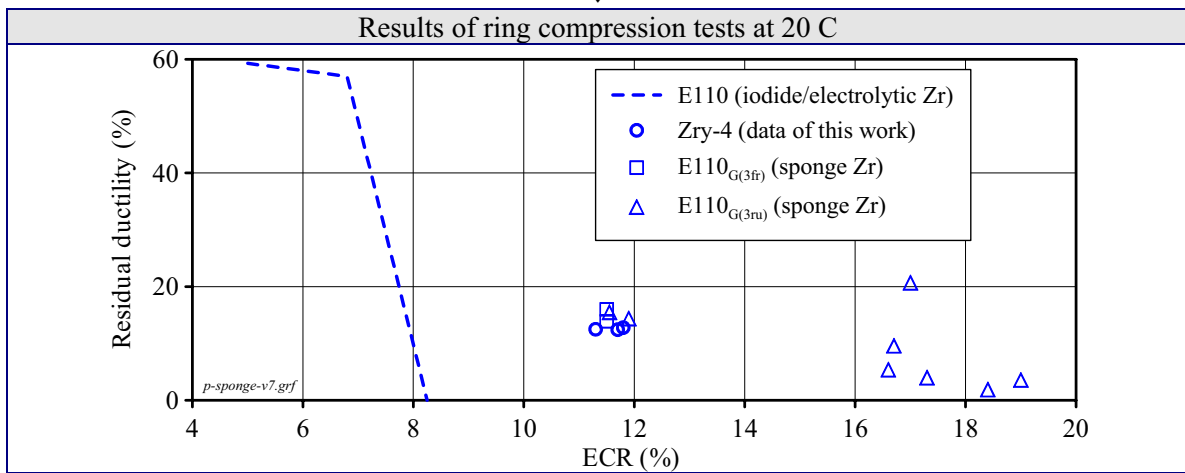


Fig. 4.9. Comparative data base characterizing the E110_{G(3fr)} and E110_{G(3ru)} oxidation/mechanical behavior

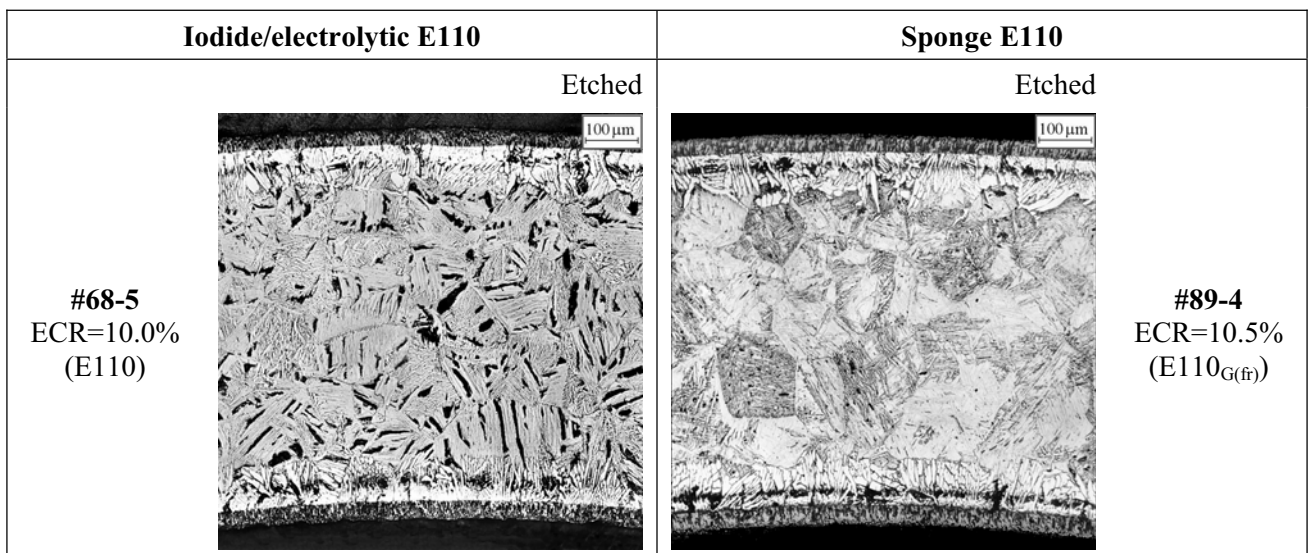


Fig. 4.10. The comparison of microstructures for iodide/electrolytic and sponge E110 claddings after the oxidation at 1100 C

Two cladding samples manufactured with the employment of electrolytic Zr with low Hf content (90 ppm) were used for this goal. The results of tests performed with these samples are presented in Fig. 4.11, in Tables B-1, B-2 of Appendix B and Fig. H-15 of Appendix H.

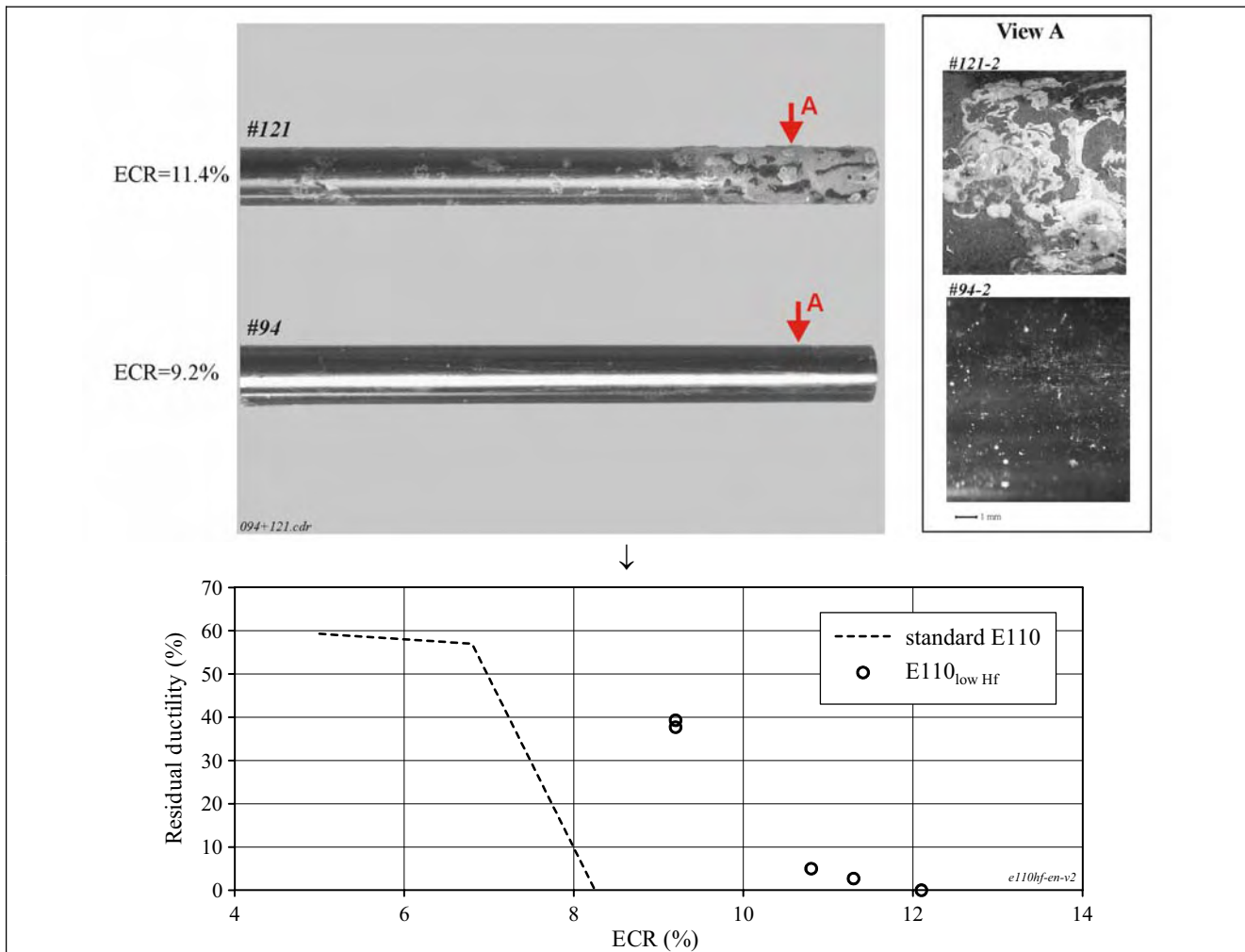


Fig. 4.11. The appearance of the E110_{low Hf} cladding after the oxidation at 1100 C and results of mechanical tests

The analysis of obtained data allows to state the following:

- the decrease of Hf content in the Zr-1%Nb alloy improves the oxidation behavior of the E110 cladding; so, the first indications of the breakaway oxidation were fixed at 9.2% ECR;
- the E110_{low Hf} sample oxidized up to 9.2% ECR has a significant margin of residual ductility and low hydrogen content (17 ppm);
- the zero ductility threshold of the E110_{low Hf} cladding is increased up to 12% ECR but the breakaway oxidation was observed in the ECR range 9-12% and the embrittlement of the E110 cladding was caused by oxygen and hydrogen pickup (the hydrogen concentration was about 430 ppm) at 11-12% ECR.

Therefore, it can be assumed that the process of electrolytic Zr cleaning of hafnium was associated with a change in the level of other chemical impurities. In this case, this change led to some improvement of the E110 oxidation behavior but not so radically as it took place for sponge types of the E110 cladding. Therefore, further investigations were continued with the E110_{G(fr)} and E110_{G(3ru)} claddings to adjust the sensitivity of the oxidation behavior of these claddings to the oxidation temperature.

4.3.3. The sensitivity of the oxidation behavior of the sponge E110 cladding to the oxidation temperature

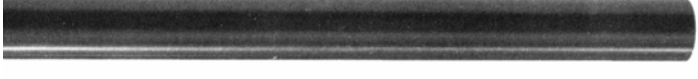
The temperature range 900–1200 C was studied in these investigations. Taking into account the results of tests with the traditional E110 cladding that showed that the oxidation behavior of the E110 alloy at 1000 C

was somewhat worse than at 1100 C, the first stage of temperature dependent tests was performed at 1000 C. These tests allowed to reveal the unexpected effect associated with a sharp decrease in the oxidation rate of the sponge type cladding at 1000 C. The scale of this effect can be characterized using the following experimental data:

- it takes 865 seconds to oxidize the standard E110 cladding up to 7.7% ECR;
- it takes 2519 seconds to oxidize the sponge type of the E110 cladding up to 6.9%;
- and it takes 5028 seconds to oxidize the sponge type of the E110 cladding up to 8.9% ECR.

The oxidation kinetics of different types for the E110 cladding will be considered in detail in the next paragraphs of the report.

As for this paragraph, the following notice concerning the oxidation rate problem should be made: a very low oxidation rate of sponge E110 cladding at 1000 C led to the fact that the time limit for the steam generator used in this test series (approximately 5000 s) was exhausted at the ECR of about 8.5–8.9%. Thus, this ECR range was the maximum one in the oxidation tests at 1000 C. The results of tests at 1000 C are presented in Fig. 4.12.

Cladding characterization		Oxidation duration	Cladding appearance
E110 (traditional)	ECR=7.7%	$t_{ef}=865$ s	#44 
E110 _{G(fr)}	ECR=6.5% (28 ppm of H content)	$t_{ef}=2016$ s	#91 
E110 _{G(3ru)}	ECR=6.9% (16 ppm of H content)	$t_{ef}=2519$ s	#98 
E110 _{G(3ru)}	ECR=8.9% (11 ppm of H content)	$t_{ef}=5028$ s	#101 
E110 _{G(fr)}	ECR=8.5% (12 ppm of H content)	$t_{ef}=5013$ s	#93 

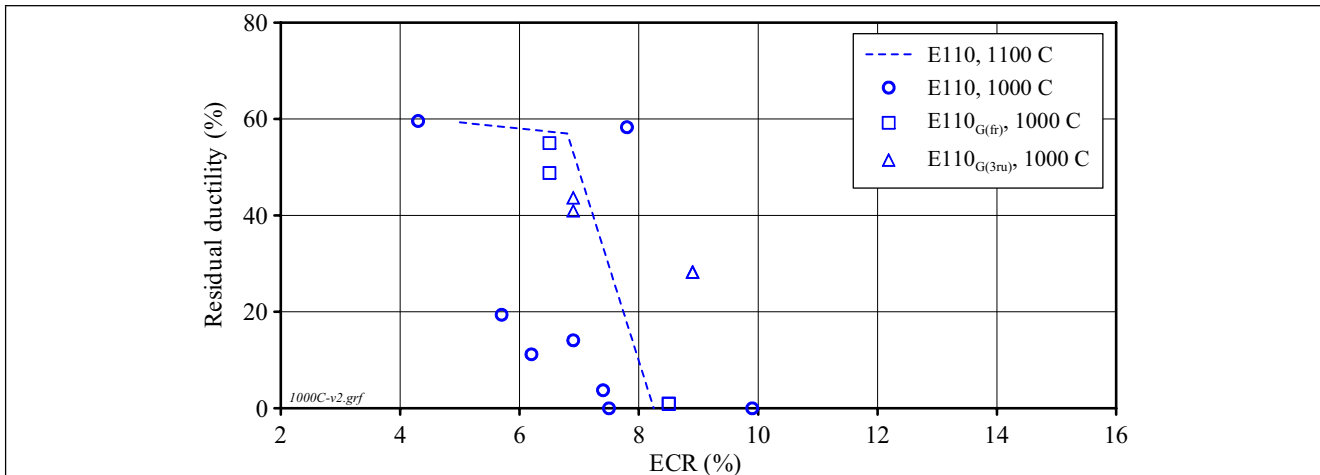
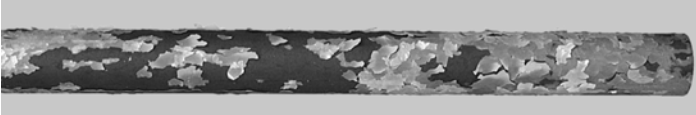


Fig. 4.12. The appearance and mechanical properties of different E110 claddings after the oxidation at 1000 C

The obtained data allow to formulate the following important observations:

- after the oxidation during 800 s at 1000 C, the E110 cladding manufactured in accordance with the traditional method of Zr-1%Nb ingot preparation has typical indications of the breakaway oxidation;
- the E110 standard cladding achieves the zero ductility threshold after the oxidation during somewhat longer than 800 s at this temperature;
- the sponge types of the E110 cladding oxidized at 1000 C during 2500 s have a significant margin of residual ductility, low hydrogen concentration in the prior β -phase, and the uniform corrosion type of oxidation;
- the first demonstration of the breakaway oxidation of the sponge E110 claddings appears after 5000 s of oxidation, hydrogen content in the cladding remains still low but the zero ductility threshold is achieved due to the decrease in the prior β -phase thickness and the increase of oxygen concentration in the cladding matrix.

Besides, the obtained data allow to formulate one new problem: for oxidation at 1000 C, the critical measured ECRs corresponded with the zero ductility thresholds of standard and sponge ECR claddings are similar to both types of the cladding but the oxidation duration differs approximately six times. In the context of this problem, the following question could be formulated: is the measured (calculated) ECR a unequivocal criterion characterizing the zero ductility conditions? The additional consideration of this issue will be continued in one of next paragraphs of the report. To investigate the sponge E110 cladding behavior at temperatures lower than 1000 C, one reference test was performed at 900 C (with modified steam generator). The results of this test are shown in Fig. 4.13.

Cladding characterization		Oxidation duration	Cladding appearance
E110 (standard)	ECR=6.7%	$t_{ef}=4804$ s	#131 
E110 _{G(3ru)}	ECR=7.5%	$t_{ef}=14400$ s	#137 

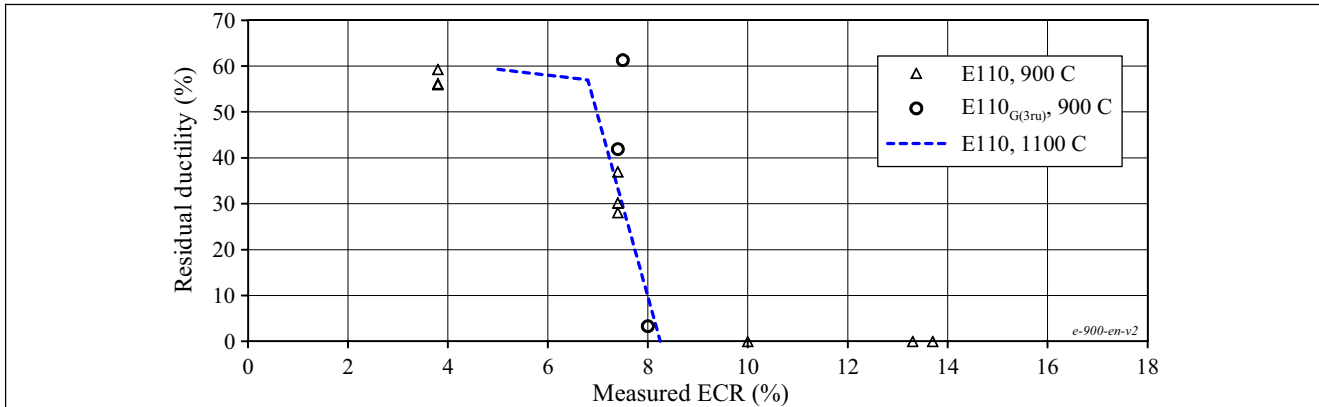


Fig. 4.13. The comparative test data characterizing the E110 and E110_{G(3ru)} behavior after the oxidation at 900 C

The present data allow to observe that general tendencies revealed for two types of the E110 cladding at 1000 C are retained at 900 C also:

- the embrittlement of the E110_{G(3ru)} cladding is not the consequence of the breakaway oxidation in contrast to the standard E110 cladding;
- much more time is needed to achieve approximately the same ECR in the sponge E110 cladding and the same margin of residual ductility as those in the standard E110 cladding (14400 s and 4800 s respectively);
- the critical measured ECR characterizing the zero ductility threshold of sponge type in the E110 cladding (E110_{G(3ru)}) at 900 C is approximately the same as that for the sponge E110 at 1000 C and the standard E110 at 1100 C (8.3% ECR) but the causes for embrittlement are different. The embrittlement of sponge E110 is caused by the oxygen induced mechanism but the embrittlement behavior of the standard E110 is determined by the combination of oxygen and hydrogen effects.

The last position of temperature dependent investigations with the sponge E110 cladding was devoted to the tests at 1200 C. The results of these tests are shown in Fig. 4.14.

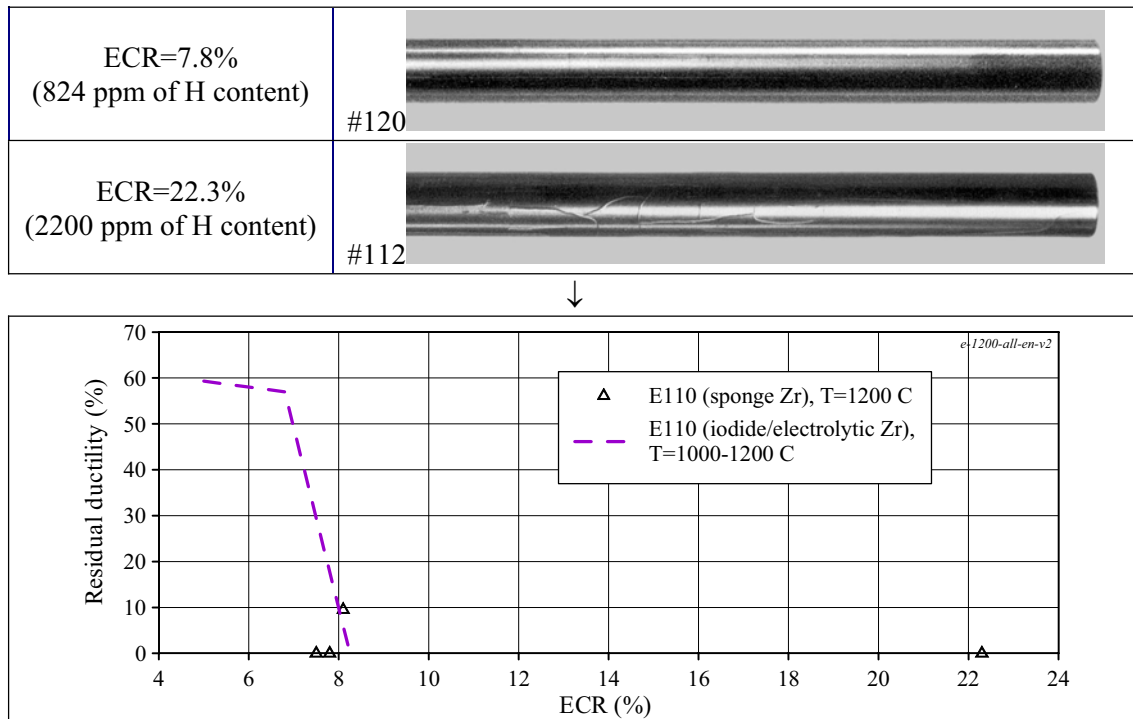


Fig. 4.14. The characterization of appearance and RT mechanical properties of the E110_{G(3ru)} cladding after the oxidation at 1200 C

The major conclusion from these test is the following: for oxidation at 1200 C, and in spite of the presence of black bright oxide on the tested cladding, the zero ductility of sponge E110 cladding of the E110_{G(3ru)} type was approximately the same as that for the standard E110 cladding. The oxidation of the E110_{G(3ru)} cladding corresponded to the significant hydrogen absorption.

Thus, the results of these tests have demonstrated that the oxidation behavior of the E110_{G(3ru)} cladding deteriorated sharply at 1200 C. In this problem, it is interesting to note that ring compression tests performed at 20 C in the ANL with Zry-4, Zirlo, M5 samples oxidized at 1200 C have shown that the residual ductility of these claddings “decreased rather abruptly from 5 to 10% ECR” [13]. These data confirm that the oxygen diffusion processes in zirconium claddings are considerably changed on proceeding from 1100 C up to 1200 C. However, the nature of these processes is not quite understood now. Besides, in spite of the similarity in the E110_{G(3ru)} behavior and Zry-4, M5, Zirlo one at 1200 C, a significant difference has been revealed also. These differences are associated with the hydrogen content in the oxidized cladding. The embrittled Zry-4, Zirlo cladding have a low hydrogen content and (on our opinion) due to this reason these claddings have demonstrated the remarkable improvement in the cladding ductility at the temperature increase in mechanical tests up to 135 C. The embrittled E110_{G(3ru)} cladding has a high hydrogen content and the temperature increase in mechanical tests up to 135 C has not led to the increase in residual ductility. In this connection, it is reasonable to assume that the revealed difference in the behavior of these claddings is associated with the fact that E110_{G(3ru)} is not 100% sponge material.

4.3.4. The analysis of results obtained in the test with the E635 cladding fabricated using sponge Zr

The E635_{G(fr)} cladding fabricated on the basis of 100% French sponge Zr was the last type of niobium-bearing claddings manufactured with the use of sponge Zr and tested in the frame of this work. These several tests were performed to extend the test data base developed to determine the sensitivity of the cladding oxidation behavior to the alloy chemical composition. The major results of tests with the E635_{G(fr)} cladding oxidized at 1100 C are presented in Fig. 4.15.

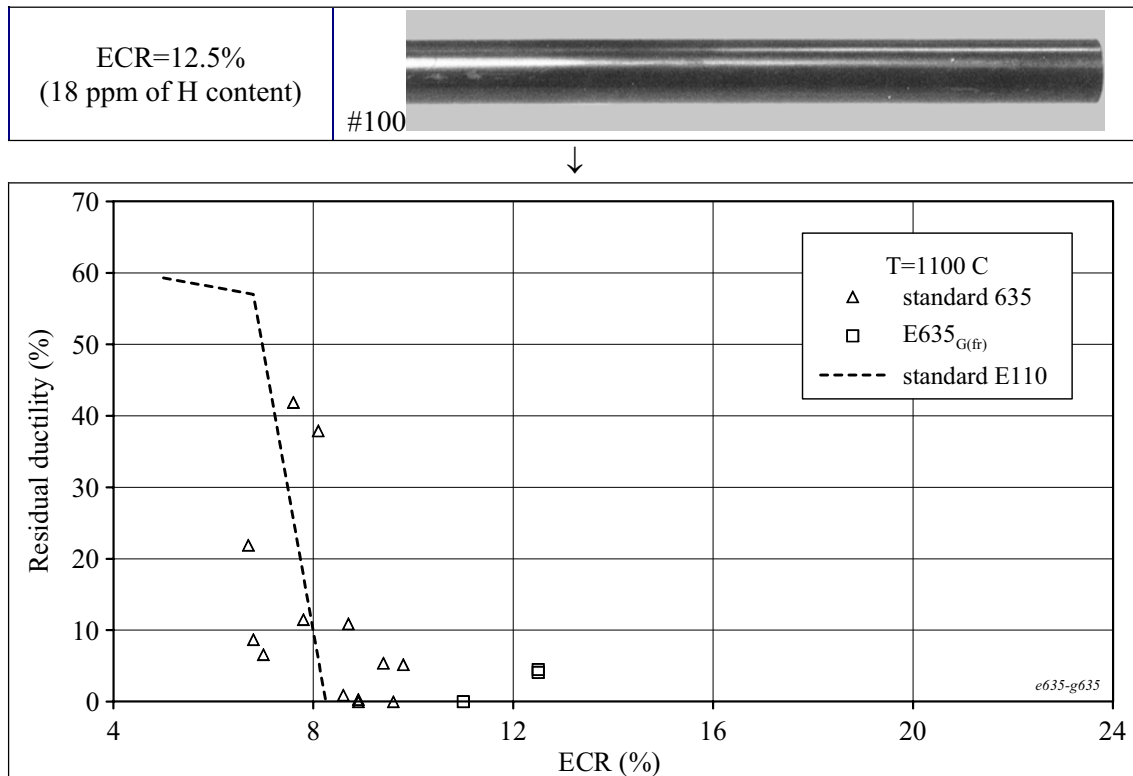


Fig. 4.15. The appearance of the E635_{G(fr)} cladding after the oxidation test at 1100 C and comparative E635 (standard), E110 (standard), E635_{G(fr)} results of ring compression tests

The obtained data allow to note the following:

- In spite of the fact that the E635_{G(fr)} oxidized cladding is characterized by a low hydrogen content in the prior β -phase up to 12.5% ECR, the first visible indications of the breakaway oxidation were observed on the cladding surface at 11% ECR;
- in contrast to sponge types of the E110 cladding, the general difference in zero ductility thresholds of the standard E635 and sponge E635 was not revealed.

4.3.5. The comparative consideration of a microchemical composition of different types of the E110 alloy

Results of tests performed with the sponge E110 cladding have demonstrated a significant improvement in the E110 corrosion resistance. To explain this phenomenon, the microchemical aspects of difference between the iodide/electrolytic E110 and sponge E110 alloys were considered. The first step in these investigations was connected with the analysis of results of previous investigations performed in this line. H.Chung developed a very interesting model for aliovalent elements specially for the interpretation of the revealed difference in the E110 and M5 alloy behavior [12]. This model is based on Wagner electrochemical theory of oxygen ions passing through oxide to the oxide/metal interface with regard to the presence of impurity and secondary phase precipitates in the cladding material [15]. The employment of this theory performed by H. Chung using the aliovalent element model in our case allowed to develop the following conception of the oxide behavior at the high temperature oxidation (>800 C) of niobium-bearing alloys:

- the impurity and alloying element should be subdivided into overvalent elements and undervalent elements in relation to the tetragonal zirconium;
- the presence of overvalent elements leads to the decrease of O⁻ vacancies and to the increase of the stoichiometric degree of oxide (a low fraction of the protective tetragonal oxide);
- undervalent elements provide:

- a high density of oxygen ions vacancies;
- the tendency towards the retention of under-stoichiometric oxide with a high fraction of tetragonal protective oxide;
- such binary alloys as the E110 and M5 contain a definite quantity of undervalent beneficial impurities: Ca, Al, Mg, Fe, Ni and a definite quantity of one overvalent alloying element Nb.

The comparative analysis of the M5 and standard E110 fabrication processes including the surface finishing performed by H. Chung led him to the following conclusions:

- both alloys have the same content of deleterious overvalent niobium;
- the M5 alloy is enriched with such beneficial elements as Ca, Al, Mg, Fe, Y during the fabrication process;
- the standard E110 alloy is enriched with such specific deleterious impurity as F during the fabrication process (electrolytic Zr production);
- the general difference in the oxidation behavior of the standard E110 and M5 alloys is caused by the differences in the above listed beneficial and deleterious impurities.

In the context of these conclusions, it should be specially noted that:

- the use of fluoride compounds during the electrolytic E110 fabrication was always the object of a special attention and control of F content during the E110 manufacturing process;
- the results obtained by V. Vrtilkova after the oxidation tests with the E110 alloy were used by H. Chung on the validation of his position in this issue [16]. However, it should be pointed out that V. Vrtilkova used the E110 tubes manufactured from iodide Zr only because only this method of the E110 fabrication was employed in Russia before 1985. But it is known that the iodide Zr contains much less impurities than electrolytic and sponge Zr;
- besides, Wagner theory could be used for the impurity elements having a significant solubility in ZrO_2 (Ca, Mg, Al, Y), but it is known that such elements as Fe, Nb, Sn are practically insoluble in ZrO_2 and these elements are present in the oxide on the crystalline grains as independent phases.

Russian investigations performed on developing the E110 alloy have shown that the most deleterious impurities in the zirconium alloys are the following: C, N, F, Cl, Si. Besides, such elements as Ti, Al, Mo, Ta, V negatively influence the corrosion resistance, the beneficial influence was revealed for Fe and Cr. The influence of major alloying elements such as Nb and Sn is not univocal. The corrosion resistance of zirconium alloys with the Nb and Sn alloying elements is the function of the content of these elements in alloys. The investigations in detail of the corrosion resistance sensitivity of Zr-Nb-based alloys and Zr-Sn-based alloys to the alloying element content performed recently confirmed this statement [9, 17]. The recent reassessment of results of autoclave corrosion tests (500 C was the maximum temperature) with the M5 cladding has shown that C (with the content >100 ppm), Al (with the content 20–150 ppm), N, Sn (with the content >100 ppm), Si (with the content >80 ppm) have a detrimental influence over the M5 corrosion behavior [7, 18]. In addition to that:

- the beneficial influence of Fe, Cr and Fe/Cr ratio over the corrosion resistance of Zr-Sn alloys was revealed [19, 20, 21, 22];
- the acceleration in the corrosion process was observed as a function of such impurities as Al, Ti, Mn, Pt, Ni, Cu in the Zr-2.5%Nb alloy [23];
- the optimal corrosion resistance was obtained for C and Fe impurities in the Zr-2.5%Nb alloy. It was revealed that the optimal content of these elements is about 30 ppm C and 1100 ppm Fe [23].

In conclusion of this overview of previous investigations, the following information concerning such elements as Nb, O, Hf may be added:

- Russian investigations on the oxygen content in the Zr-Nb alloy of 400–1000 ppm and French investigations on the oxygen content in the Zr-Nb alloy of 900–1800 ppm [18] have shown that the oxygen concentration has the negligible influence over the corrosion resistance of niobium-bearing alloys;
- the same investigation and results of investigations published in [9] allow to consider that the corrosion behavior of niobium-bearing alloys is not sensitive to the variations of Nb content in the alloy in the range 0.9–1.1 wt%;
- the role of hafnium is not completely clarified now but this element is usually considered as neutral.

Unfortunately, the comparative analysis in detail of this research results with results of previous investigations devoted to the relationship between the microchemical composition of niobium-bearing alloys and the corrosion behavior of these alloys allow to formulate the only following general conclusions:

1. The high corrosion resistance of Zr-Nb alloy under operating conditions (a low temperature range) is the necessary requirement for this type of zirconium cladding but this requirement fulfillment does not guarantee that the alloy will demonstrate a high corrosion resistance under LOCA relevant conditions (a high temperature range) also.
2. In spite of the numerous investigations performed in this line, the nature of the relationship between the corrosion resistance and chemical composition of the alloy is not quite understood yet.

Taking into account these conclusions, the plan for comparative studies of the chemical composition of the iodide/electrolytic E110 and sponge E110 was developed on the basis of the following major provisions: the measurement results of the standard E110 alloy chemical composition (used for our oxidation tests) and measurement results of sponge types of the E110 alloy chemical composition (tested during this program) must be compared. Reasonable differences in the content of chemical elements should be revealed and analyzed.

At the first stage of this plan, a typical content of the E110 alloy presented in Table 4.4 was compared with a real content of chemical elements in each batch of tested E110 alloy. This comparison showed that the typical composition of the E110 alloy was representative for the tested E110 material except for Fe content. Real Fe content in the E110 alloy used for this program was 86 ppm.

Table 4.4. Chemical composition of the E110 alloy (standard) [5]

Typical content (ppm)	Chemical element												
	Al*	B	Be	C	Ca	Cd	Cl	Cr	Cu	F	Fe	H	Hf
	<30	<0.4	<30	<40-70	<100	<0.3	<7	<30	<10	<30	140	4-7	300-400
Typical content (ppm)	K	Li	Mn	Mo	N	Ni	O	Pb	Si	Sn	Ti	Nb	
	<30	<2	<3	<30	<30-40	<30-39	500-700	<50	46-90	<100	<30	0.95-1.1 wt%	

* Concentrations marked as <30, ... reflect that fact that the real concentration of elements was not measured, because it was less than the low threshold of the detector (procedure) sensitivity

At the second stage of the research, chemical compositions of the E110_{G(fr)}, E110_{G(3fr)}, E110_{G(3ru)} alloys were compared with the standard E110 composition. The comparative analysis of the appropriate data allowed to establish the reasonable difference in the impurity contents for Fe and Hf only. Nevertheless, other several beneficial and deleterious elements were added into the comparative results presented in Fig. 4.16. It should be noted that in spite of the fact that Hf influence over the corrosion resistance is not understood, we attributed this element to deleterious impurities taking into account:

- results of tests with the E110_{low Hf} cladding;
- the fact that Hf stabilizes the monoclinic oxide at higher temperatures.

By the way, the comparative analysis of the E110_{low Hf} and standard E110 cladding chemical compositions showed that the impurity contents in these materials were the same except for Hf content.

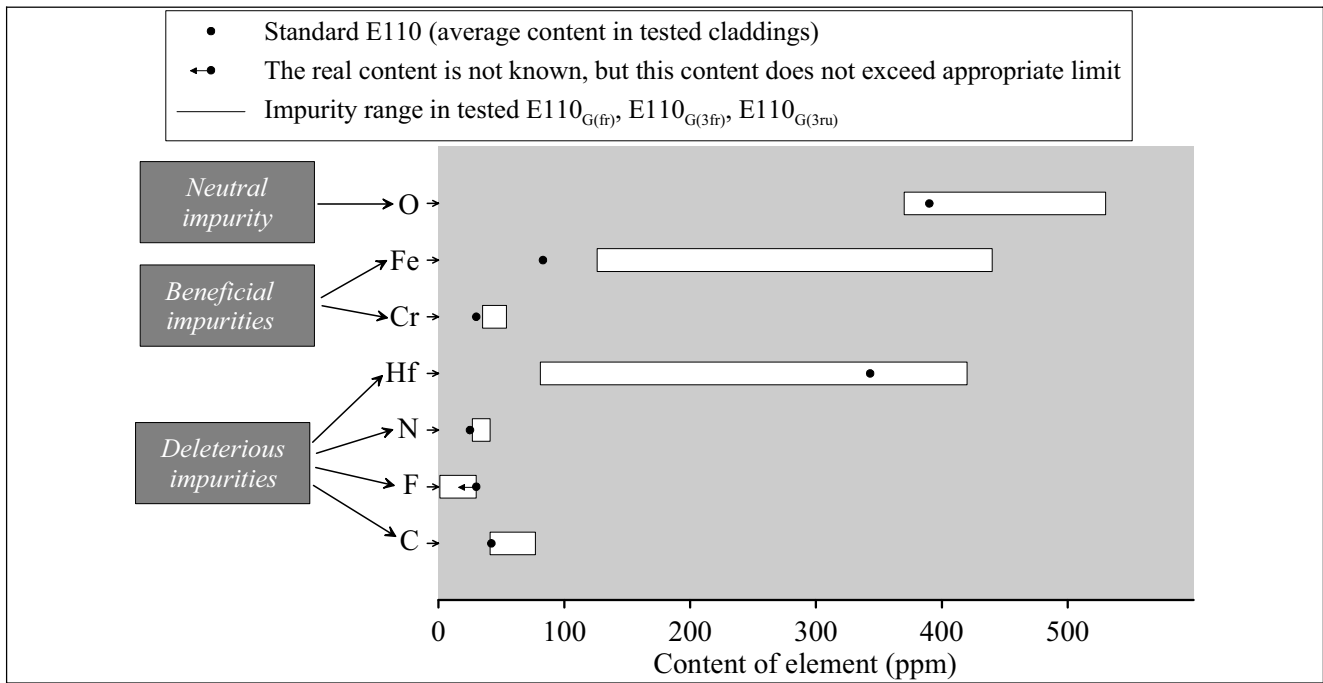


Fig. 4.16. Comparison of some data on the impurity content in the standard E110 and E110_{G(fr)}, E110_{G(3fr)}, E110_{G(3ru)} at the beginning of the cladding fabrication

Thus, the obtained data showed that one significant difference in the standard E110 and sponge E110 chemical composition was observed: Fe content in the sponge E110 is higher than that in the standard E110. But the beneficial effect of iron on the corrosion behavior of zirconium alloys is known for a long time. Therefore, the majority of alloys including such Russian alloy as E635 have a high or quite high Fe content (see Table 4.5). In this case, such alloys as Zircalys, Zirlo and E635 employ iron as the alloying element.

Table 4.5. Composition of zirconium alloys used in reactor fuel design [24]

Element	Zircaloy-4	ZIRLO	E635	M5	E110
Nb (wt%)	–	0.9–1.3	0.95–1.05	0.8–1.2	0.95–1.05
Sn (wt%)	1.2–1.7	0.9–1.2	1.2–1.3	–	–
Fe (wt%)	0.18–0.24	0.1	0.34–0.40	0.015–0.06	0.006–0.012
Cr (wt%)	0.07–0.13	–	–	–	–
Zr	Balance	Balance	Balance	Balance	Balance

The results obtained during this research confirm the important role of iron in the cladding oxidation behavior. This thesis is based on the fact that sponge types of the E110 cladding with the higher content of iron demonstrate the better corrosion behavior than the standard E110 alloy with low Fe content as well as on the fact that the results of oxidation tests of the E635 cladding (iodide/electrolytic) with a very high content of iron have shown that the oxidation behavior of the standard E635 cladding is somewhat better than that of the standard E110 cladding. Though, in this case the absence of a general difference in the oxidation behavior of the standard E635 and sponge E635 impels to involve additional test data to continue the analysis of this and other issues connected with the chemical composition of Zr-Nb alloys. The interesting scope of investigations was recently performed in the VNIINM (Russia) [25].

Seven types of niobium-bearing claddings (iodide/electrolytic) were oxidized at 1100 C and mechanically tested. These seven types of the cladding are characterized by the following range of chemical composition variations:

- Nb → 0.9–11 wt%;

- Fe → 80–1400 ppm;
- C → 45–200 ppm;
- Hf → 100–430 ppm;
- Cr → 30–60 ppm;
- O → 350–1300 ppm.

The analysis shows that these claddings have demonstrated quite different oxidation and mechanical behavior. These types of this behavior and appropriate contents of chemical elements in the cladding material are characterized in Table 4.6.

Table 4.6. The organized results of oxidation and mechanical tests with seven types of the standard E110 and modified E110 (the data of [25])

Test parameters	Corrosion resistance at 10% ECR		
	Best	Intermediate	Worst
The cladding sample number	##2, 3, 4	##5, 6	##1, 7
The corrosion type	Uniform (lustrous black protective oxide)	Beginning of the nodular oxidation (white spots on the cladding surface)	Typical breakaway oxidation. The spallation of white oxide
Hydrogen content (ppm)	60–200	200–400	400–600
Mechanical properties	Maximum residual ductility and fracture energy	Very low residual ductility and fracture energy	Very low residual ductility and fracture energy
The impurity content (ppm):			
Fe	130–450	80–1400	100–140
O	350–600	890–1300	350–500
C	<45–65	70–200	60–80
Hf	100–430	360–370	100–360
Cr	<30–60	<30	<30

The consideration of the data presented in Table 4.6 shows that:

- the cladding with the iron content of about 130–450 ppm having relatively low C content and low Hf content (~100 ppm) have demonstrated the best corrosion resistance;
- the intermediate corrosion resistance was observed at very low and very high Fe content (80 and 1400 ppm) and high Hf content, in this case, the direct sensitivity to the C content in the range of 70–200 ppm was not revealed;
- the relationship between the worst corrosion resistance and the concentration of chemical elements listed in Table 4.6 is not quite understood.

The analysis of these results performed by the VNIINM researchers led them to the assumption that the oxidation behavior of the E110 alloy is not so much the function of Fe, C, ... concentration as the function of the quantity of impurities in the alloy. Special measurements performed for this goal showed the following [25]:

- the sum of Ni, Al, Si, Ca, K, F, Cl, Na, Mg impurities in the E110 cladding, having the intermediate and worst corrosion behavior was about 110–135 ppm;

- the appropriate sum in the E110 claddings that demonstrated the best corrosion behavior was about 25–45 ppm, in this case, the corrosion resistance decreased as impurity contents increased from 25 up to 45 ppm.

Unfortunately, it was impossible to perform the comparison of this type for impurity contents in the standard E110 and sponge E110 on the basis of data presented in Table 4.4 and in the Fig. 4.16. The thing is that the methods used to measure the concentration of very many impurities allowed to guarantee that the concentration of some impurity was not higher than the value presented in Table and Figure (<30, <40, ...). However, these methods did not allow to measure the real impurity concentration in the alloy. It was also impossible to estimate the impurity contents in the M5 alloy because these data were not published. But some additional data useful for the analysis of this issue could be taken into account from the consideration of impurity contents in Zirlo presented in Table 4.7.

Table 4.7. Chemical composition of the Zirlo cladding tube [26]

Element content (ppm)	Chemical element																
	Al	C	Cr	Cu	Hf	Fe	Mg	Mo	Ni	Nb	N	O	Si	Sn	Ti	W	Zr
	120	20	10	20	<40	1000	<10	<10	<10	1.23 wt%	50	1450	130	1.08 wt%	19	<40	Bal- lan- ce

A special comment must be done before the analysis of these data:

- chemical compositions of the E110 alloy presented in Table 4.4, Table 4.6 characterize the ingot compositions;
- the E110 chemical compositions presented in Fig. 4.16 characterize the beginning of the cladding fabrication processes;
- special measurements of the E110 overall impurity contents were performed in the unoxidized E110 tubes;
- the Zirlo composition presented in Table 4.7 was measured using the Zirlo tubing.

Thus, the cladding tubes were used in both cases for the measurement of the sum of the E110 impurity content and Zirlo impurity content. The comparison of appropriate data showed that the hypothesis proposed in [25] to explain the E110 oxidation behavior on the basis of the sum of impurity contents was not confirmed as applied to the Zirlo claddings. So, the sum of two impurities only (Al and Si) is 250 ppm in the Zirlo cladding. But the oxidation behavior of the Zirlo cladding is characterized by the uniform corrosion and low hydrogen concentration in accordance with the data obtained in the ANL. Though, on the other hand, some data characterizing the content of impurities in the M5 alloy is in a good agreement with the assumption about the fact that the optimization of the content of beneficial impurities does not allow to achieve a high corrosion resistance at a high overall concentration of other impurities in the alloy. So, these some data characterizing the M5 alloy are the following [7, 18]:

- the sum of Ca, Mg, Sn, S contents in the alloy is less than 1 ppm;
- the sum of Si, Zn, Al contents in the alloy is less than a few ppm;
- the C content is 25–120 ppm.

Besides, these data characterizing the chemical composition of the M5 alloy allow to return to the discussion of the fact that the electrochemical theory of the cladding oxidation and the model of aliovalent elements (developed on the basis of this theory) must be added with models taking into account other competing processes in the niobium-bearing claddings under high temperature oxidation conditions.

If the experimental and analytical data presented in this paragraph are generalized then the following conclusions may be made:

- the cladding high temperature oxidation behavior has a series of peculiar features associated with the phase compositions and temperature dependent characteristics of the solubility and diffusion of alloying and impurity elements in the oxide and metallic matrix. Therefore, the studies of these processes should be performed under high temperature conditions. A direct transfer of results for low temperature corrosion tests to the high temperature corrosion behavior may result in grand errors;
- the impurity composition is one of the key factors determining the oxidation behavior of Zr-Nb alloys at high temperature conditions;
- there is a serious reason to change the current approach from the classification of impurities by the beneficial and deleterious ones to the following approach:
 - minor alloying elements (this term was proposed in [23]), these are impurities allowing to provide the uniform mechanism of oxidation and to minimize the hydrogen content in the oxidized cladding; the requirements for the content of these elements must be developed;
 - deleterious impurities for which the requirements must be stipulated for their individual content in the alloy or the requirements for their total content in the alloy;
 - neutral impurities; the concentration of these impurities in the alloys in the current limits do not affect the oxidation mechanism and oxidation rate.

As for the E110 alloy, the list of impurities in accordance with this new classification cannot be determined basing on the results of this research. But it seems that iron is the first candidate for the incorporation into the set of the E110 minor alloying elements.

4.4. The comparative analysis of the E110 material microstructure

As it was reported at the beginning of this section, the bulk effects (in the context of the cladding oxidation behavior) are considered on the basis of two independent experimental data bases:

1. The data base characterizing the dependence of the cladding oxidation behavior in a function of the cladding material chemical composition.
2. The data base characterizing the dependence of the oxidation phenomena in a function of the cladding microstructure.

In our case, the microstructure investigations with samples from different types of the E110 cladding were especially urgent because of the fact that the analysis of results obtained in microchemical investigations presented in the previous paragraph did not allow to develop the unequivocal explanation of the E110 specific behavior.

The program for special TEM examinations was worked out to determine the following comparative data characterizing the microstructure of tested claddings:

- phase conditions and phase compositions;
- the grain size in the cladding matrix;
- the characterization of the secondary phase precipitates including: the chemical composition, size, density, the character of precipitates' distribution.

The following as-received tube samples were used for this research:

- standard E110;
- E110_{G(fr)};
- E110_{low Hf}.

The basic examinations were performed in the RIAR using the transmission electron microscope JEM-2000 FX II at the acceleration voltage 120 kV.

Taking into account that results of numerous investigations performed recently with different claddings showed a strong dependence of the corrosion resistance on parameters of intermetallic precipitates in the alloy, the examinations in detail of precipitates were carried out using thin foils and carbon replicas.

The comparative data characterizing TEM images of different E110 claddings are presented in Fig. 4.17 together with the M5 TEM image reprinted from [27]. The analysis of visual observations obtained after studies of this information has shown that:

- all presented cladding samples have the equiaxed α -Zr grains and globular secondary phase particles (SPP) uniformly distributed in the α -Zr matrix (see also Fig. 4.18);
- the microstructure of all cladding samples is completely recrystallized.

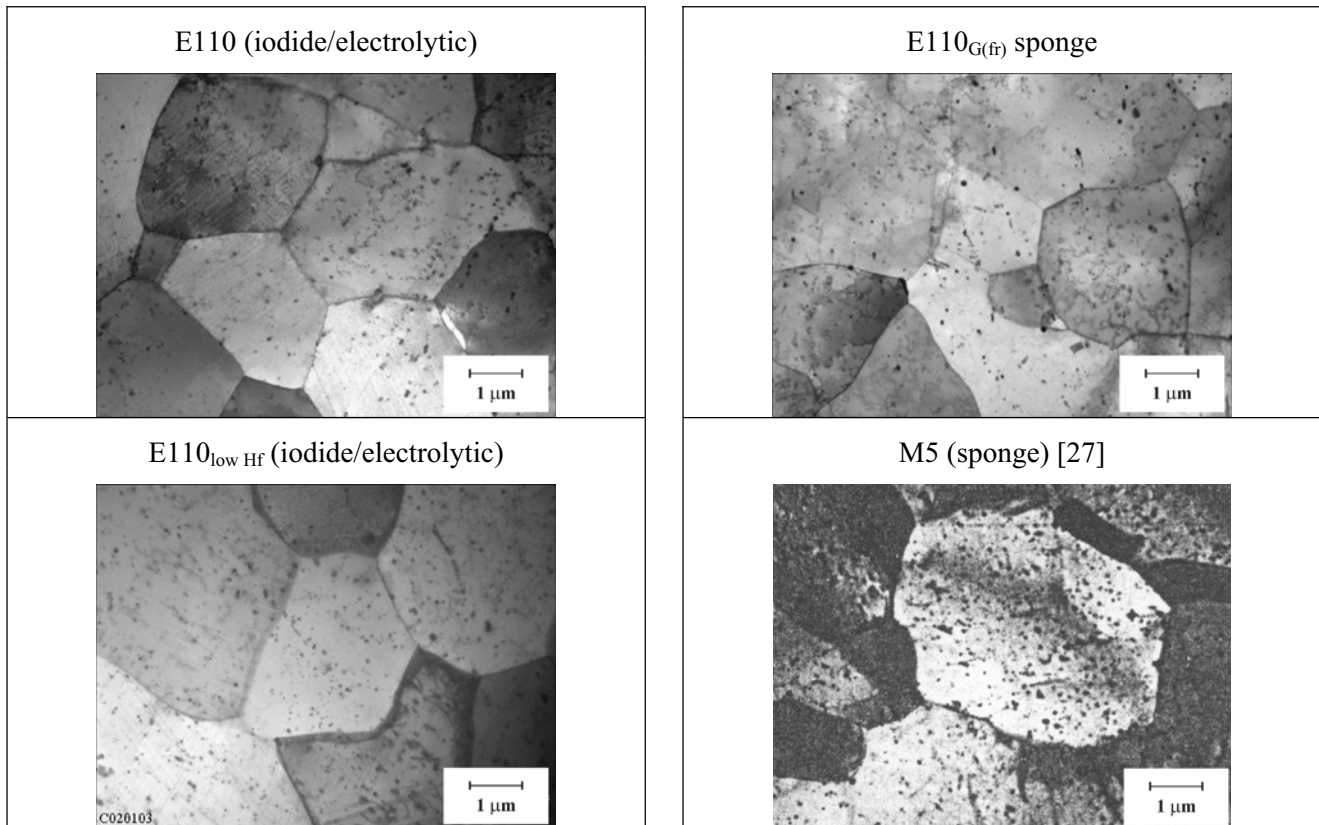


Fig. 4.17. Low magnification of TEM micrographs for E110, E110_{G(fr)}, E110_{low Hf} claddings and the M5 cladding [reprinted from 27]

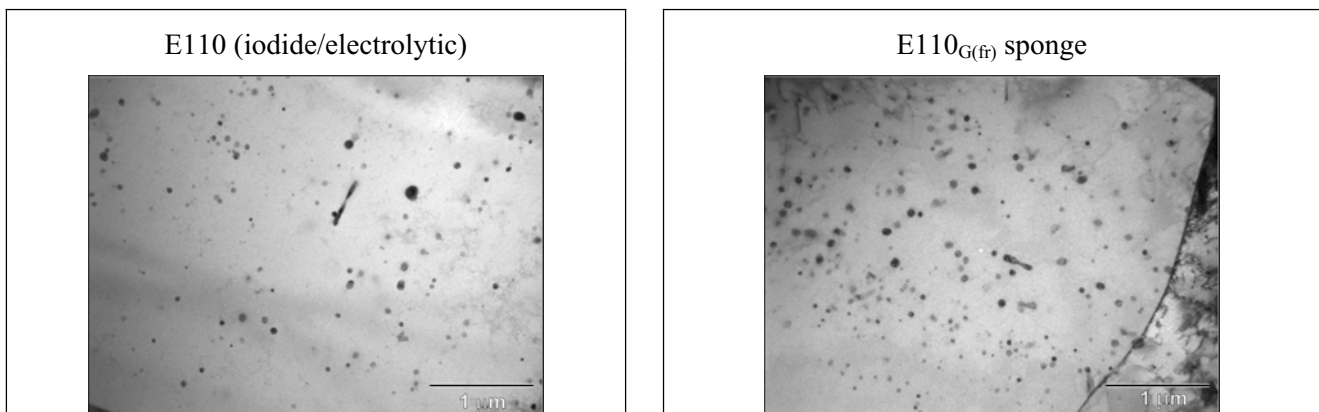


Fig. 4.18. The characterization of the SPP distribution in the α -Zr grains of the E110 and E110_{G(fr)} claddings

The next stage of examinations was devoted to the determination of the α -Zr matrix chemical composition, the grain boundary and SPPs. The energy dispersion X-ray analysis (EDX) was employed for these quantitative measurements. Besides, the SPP sizes and SPP density were measured also.

The measured chemical compositions of the α -Zr matrix and β -Nb precipitates in different E110 claddings are presented in Table 4.8.

Table 4.8. Zr, Nb content in the matrix, grain boundary and β -Nb precipitates

Element	Concentration (wt%)								
	Matrix			Grain boundary			β -Nb		
	E110	E110 _{low Hf}	E110 _{G(fr)}	E110	E110 _{low Hf}	E110 _{G(fr)}	E110	E110 _{low Hf}	E110 _{G(fr)}
Zr	99.59 \pm 0.97	99.34 \pm 1.03	99.51 \pm 1.17	99.54 \pm 1.11	99.62 \pm 0.92	99.54 \pm 1.14	11.03 \pm 1.17	9.66 \pm 0.48	11.49 \pm 0.65
Nb	0.41 \pm 0.26	0.66 \pm 0.28	0.49 \pm 0.31	0.46 \pm 0.29	0.38 \pm 0.26	0.46 \pm 0.32	88.97 \pm 2.68	90.34 \pm 1.19	88.51 \pm 1.56

The analysis of obtained data showed that no significant differences regarding Zr and Nb content in the microstructure components of E110, E110_{G(fr)}, E110_{low Hf} claddings were revealed. It is known that the best corrosion resistance is observed in the cladding material with fine α -Zr grains and fine β -Nb precipitates distributed uniformly. Therefore, the next task of TEM examinations was focused on measurements of SPP size distributions and on the determination of the average size for α -Zr grains and intermetallic precipitates.

The results of appropriate measurements allowed to reveal the following:

- the α -Zr average grain size in the tested cladding materials was very similar (2.8–3.2 μ m);
- the average size of secondary precipitates was similar also (43–48 nm), SPP size distributions in the E110, E110_{G(fr)}, E110_{low Hf} samples are presented in Fig. 4.19;
- the SPP density was about $1.8 \times 10^{20} \text{ m}^{-3}$.

To improve the representativity of TEM data obtained in the RIAR with the use of a very limited number of samples, the independent TEM investigations were performed in another Russian scientific institute (Institute of Reactor Materials) also. The results of these examinations are in a good agreement with the RIAR data except for the SPP average size in the E110 cladding which was determined as 60 nm. The SPP average size in E110_{low Hf} and E110_{G(fr)} claddings were estimated as 55 and 41 nm, respectively.

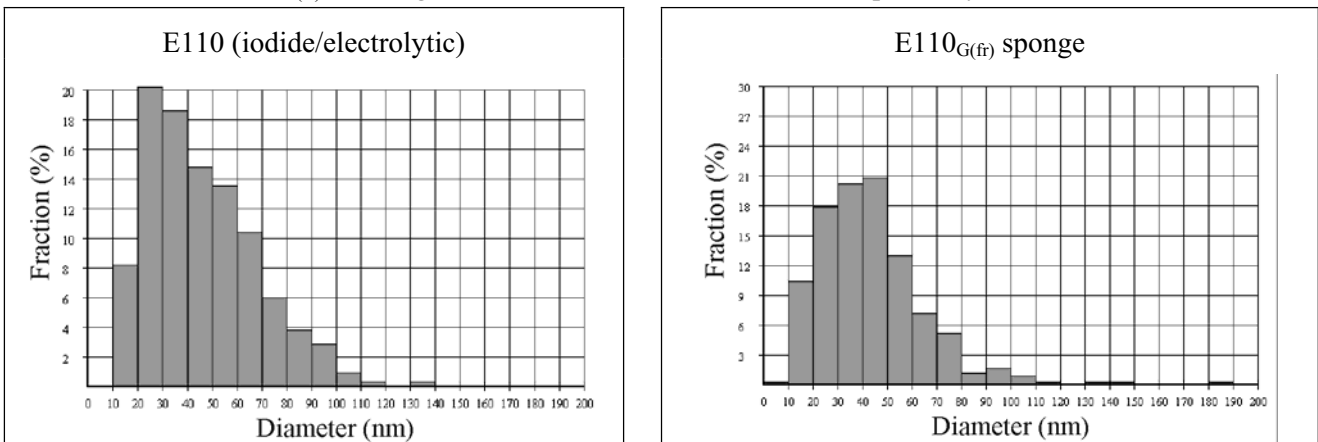


Fig. 4.19. The SPP distribution in the E110 and E110_{G(fr)} claddings

The analysis of TEM micrographs and TEM SPP distributions allowed to reveal the following general differences in the E110 (E110_{low Hf}) and E110_{G(fr)} cladding microstructures:

- the E110 cladding contained only one type of secondary precipitates, this is a beta-phase particle enriched with niobium (86–91%);

- the E110_{G(fr)} cladding contained (in addition to β -Nb precipitates) the intermetallic phase of the Zr(Nb,Fe)₂ type (see Fig. 4.20) with the average size 180 nm.

To compare the obtained TEM results, the organized data base with parameters of iodide/electrolytic and sponge E110 was developed and presented in Table 4.9. Taking into account the limited number of TEM examinations performed in the frame of this work, the E110 data were added with the results of VNIINM investigations [25]. Besides, the published data on the M5 cladding [7] were incorporated in this Table also.

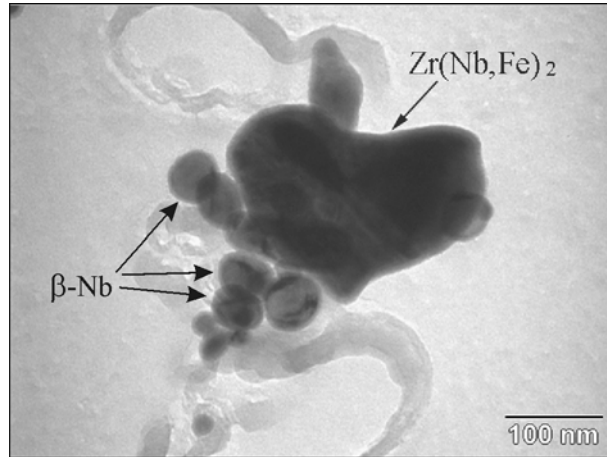


Fig. 4.20. High magnification of the SPP TEM micrograph in the E110_{G(fr)} cladding

Table 4.9. The comparative data characterizing the microstructure of E110, E110_{G(fr)} claddings and the M5 cladding [7]*

List of parameters	Cladding type		
	E110 (iodide/electrolytic)	E110 _{G(fr)} (sponge)	M5 (sponge)
1. Intermediate and final annealing temperature (C)	580	580	580
2. The phase state due to the thermal treatment	The fully recrystallized microstructure (α Zr+ β Nb)	The fully recrystallized microstructure (α Zr+ β Nb)	The fully recrystallized microstructure (α Zr+ β Nb)
3. The type of α -Zr grain	Equiaxed	Equiaxed	Equiaxed
4. The average size of α -Zr grain (μ m)	<ul style="list-style-type: none"> 2.8 (this work) 4–4.5 [25] 	3.2	3–5
5. The characteristics of β -Nb precipitates:			
<ul style="list-style-type: none"> the geometrical form 	Globular	Globular	Globular
<ul style="list-style-type: none"> the average size (nm) 	45–60 (this work) 50 [25]	41–43	45
<ul style="list-style-type: none"> the distribution density (cm^{-3}) 	$1.84 \cdot 10^{14}$	$1.8 \cdot 10^{14}$	$1.5 \cdot 10^{14}$
6. The intermetallic precipitates:			

* The all data characterizing the M5 cladding was taken from [7]

List of parameters	Cladding type		
	E110 (iodide/electrolytic)	E110 _{G(fr)} (sponge)	M5 (sponge)
• the type	–**	Zr(Nb,Fe) ₂	Zr(Nb,Fe,Cr) ₂
• the size (nm)	–	180	100–200

The analysis of comparative data allows to conclude the following:

- the most of the key parameters characterizing the cladding microstructure are practically the same in the E110 (E110_{low Hf}), E110_{G(fr)} and M5 claddings;
- the major and the only revealed distinction between the E110 and E110_{low Hf} claddings and the E110_{G(fr)} and M5 claddings regards to the absence of iron-based precipitates in the cladding material. Some distinction between the chemical composition of intermetallic SPPs in the E110_{G(fr)} and the M5 alloy (Zr(Nb,Fe)₂ and Zr(Nb,Fe,Cr)₂, respectively) may be associated with an insufficient scope of appropriate measurements performed in the E110_{G(fr)} samples.

The revealed differences in the presence and absence of iron-based precipitates are in the complete agreement with the results of microchemical investigations presented in the previous paragraph and with the data characterizing the iron solubility limit in zirconium claddings. This limit is about 100 ppm. Taking into account that iron content in the E110 alloy is about 90 ppm, it is fully dissolved in the zirconium matrix. Iron concentration in the sponge types of the E110 cladding is in range 130–430 ppm. Therefore, one part of iron is dissolved in the matrix and the second part is presented as the intermetallic precipitates. As it was mentioned in the previous sections of the report, the most of the appropriate investigations have demonstrated a high importance of intermetallic precipitates in the oxidation behavior of zirconium cladding. Moreover, it was revealed that the iron-based precipitates improve significantly the corrosion resistance and reduce H uptake.

But the analysis of this research data and data obtained in the VNIINM [25] allows to assume that there is an optimal content of iron in the alloy with which the best corrosion behavior is observed. Lower and higher Fe concentrations deteriorate the corrosion resistance.

The following general conclusions may be made on the basis of the whole scope of obtained results:

- the differences in the oxidation behavior of the standard E110 and sponge-based E110 claddings are not a function of the cladding fabrication;
- the differences in microchemical compositions of impurities are probably the major factor for the different oxidation behavior of these types of the E110 claddings;
- more careful measurements of the chemical composition of impurities especially such as C, N, F and other nonmetallic deleterious impurities must be performed in the future to adjust these phenomena;
- additional investigations must be performed also to adjust Hf and Cr influence;
- special experimental investigations with the E110 cladding containing different Fe contents may also be useful for the determination of the optimal Fe concentration.

4.5. The oxidation kinetics of the sponge type E110 cladding

The oxidation tests with the E110 claddings manufactured on the basis of sponge Zr showed that the oxidation kinetics for the standard iodide/electrolytic and sponge E110 cladding was similar, though some tendency towards the increase of oxidation rate was observed for the sponge type E110 cladding in the temperature range 1100–1200 C (see Fig. 4.21). These results are in the good agreement with the published data characterizing the oxidation kinetics of the M5 cladding [18].

** The iron-based intermetallic precipitates was not observed in the E110 cladding

Unexpected results on the oxidation kinetics of the sponge E110 were obtained in the temperature range 900–1000 C. In accordance with experimental results presented in Fig. 4.22, the oxidation rate of the sponge E110 was much less than that of the standard E110. The comparison of the sponge E110 behavior with the M5 behavior demonstrated the same effect for this alloy also.

The processing of data base characterizing the oxidation kinetics of the E110_{G(fr)}, E110_{G(3fr)}, E110_{G(3ru)} claddings allowed to develop the approximation for the oxidation rate of the sponge type E110 claddings as a function of the reciprocal oxidation temperature. The comparative data on the oxidation rate of two types of the E110 cladding are presented in Fig. 4.23.

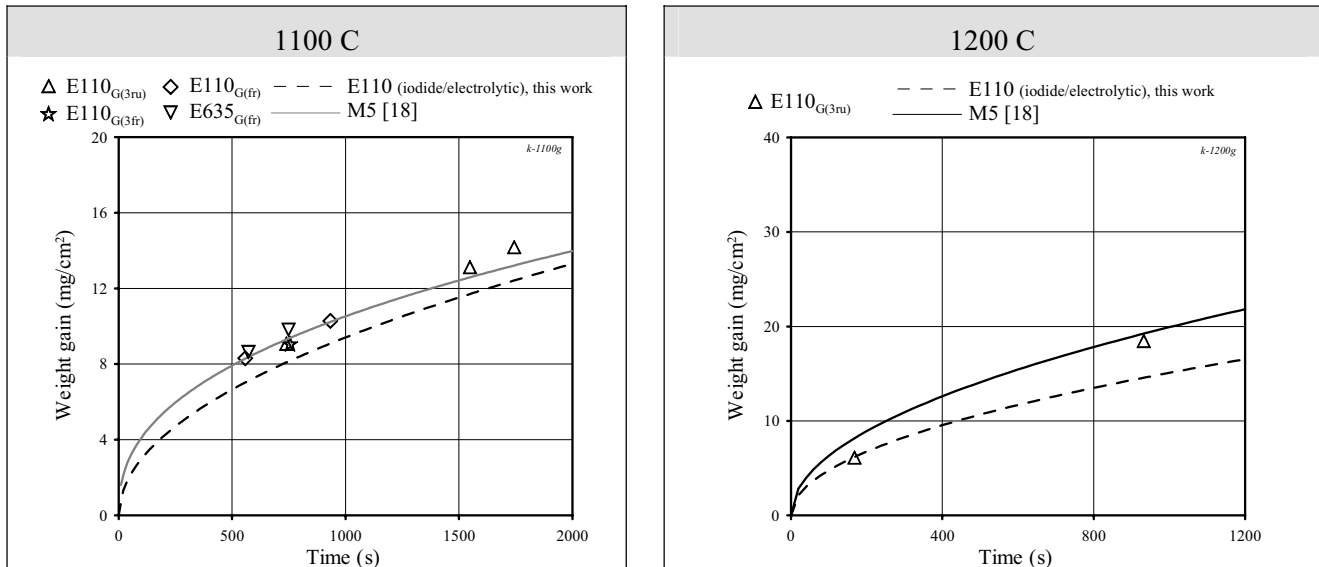


Fig. 4.21. The oxidation kinetics of different types of Zr-1%Nb claddings at 1100 and 1200 C

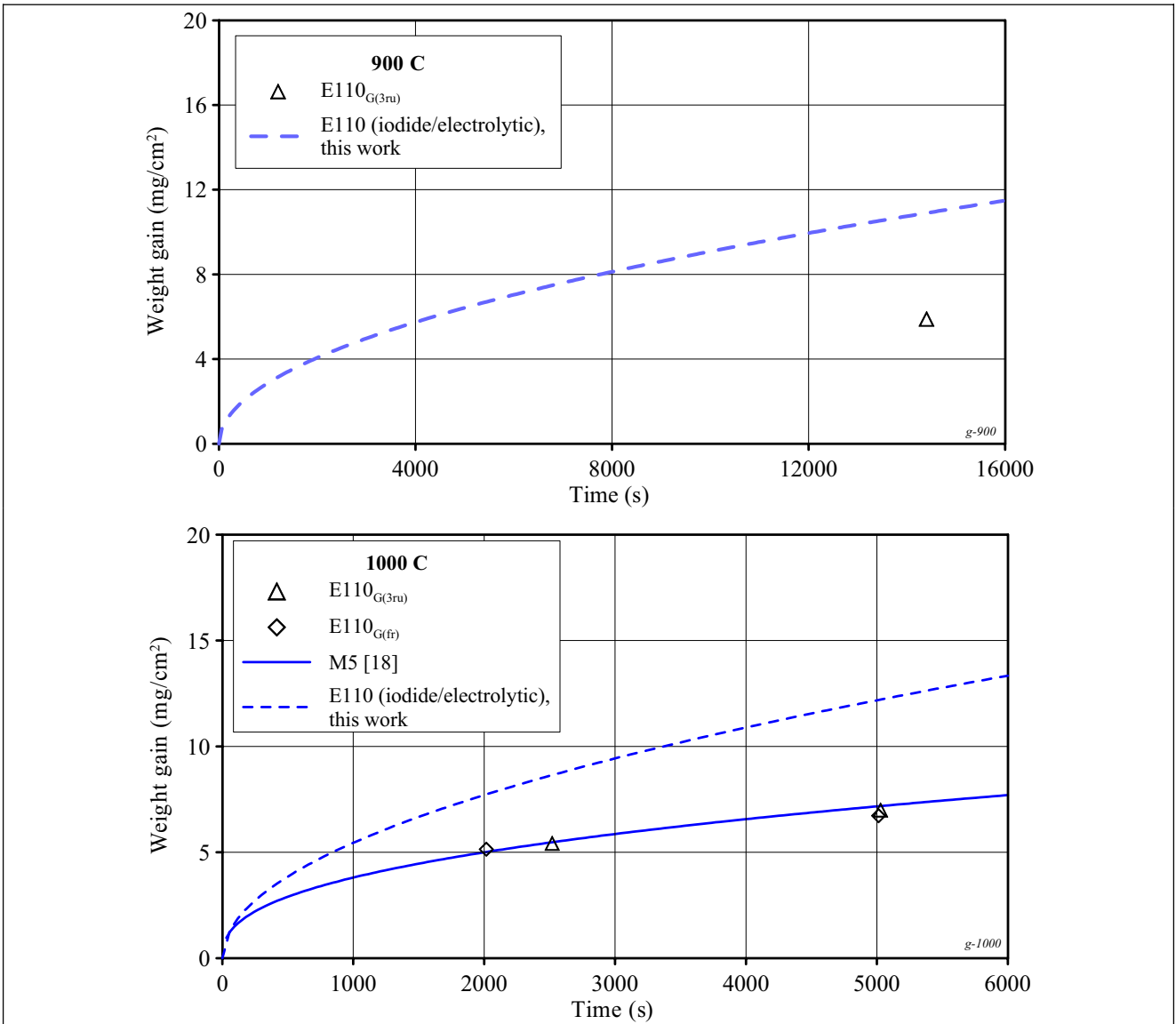


Fig. 4.22. The oxidation kinetics of different types of Zr-1%Nb claddings at 900 and 1000 C

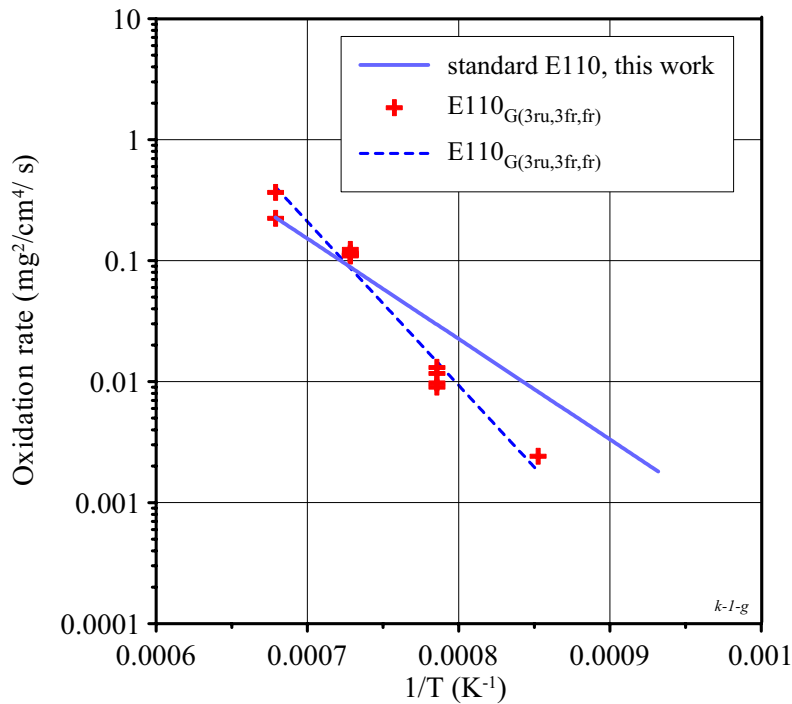


Fig. 4.23. The characterization of the oxidation rate for the standard E110 (iodide/electrolytic) and E110 claddings manufactured with the use of sponge Zr in the temperature range 900–1200 C

This effect was adjusted basing on the analysis of the following microstructural characteristics of the oxidized cladding:

- the comparison of ZrO_2 and α -Zr(O) thicknesses formed in the iodide/electrolytic and sponge E110 during the oxidation at 1000 C (Fig. 4.24);
- the comparison of ZrO_2 and α -Zr(O) thicknesses formed in the sponge type E110 cladding during the oxidation at 1000 and 1100 C (Fig. 4.25).

The procedure of these studies was complicated by the fact that metallographic samples prepared from the standard E110 claddings oxidized at 1000 C are characterized by a partial or complete loss of ZrO_2 layer. The oxide flake off occurred during the oxidation post-oxidation manipulations (including cutting of the oxidized cladding on preparing the metallographic sample). Nevertheless, the consideration of appropriate metallographic samples allowed to select the fragment of the polished sample with the representative thickness of ZrO_2 and the fragment of the etched sample for the estimation of α -Zr(O) thickness (see Fig. 4.24).

The analysis of this data allowed to reveal a general difference in two main competing processes, which define the oxygen uptake by the zirconium cladding: oxygen uptake during the oxidation of a relatively narrow surface layer still to ZrO_2 and the oxygen uptake due to the oxygen transport into the cladding depth with the formation of α -Zr(O) layer. The comparative data presented in Fig. 4.24 show that ZrO_2 is thicker and α -Zr(O) is thinner in the iodide/electrolytic E110 than those in the sponge E110 at approximately the same weight gain. The similar case is observed at the comparison of the sponge E110 oxidized at 1100 C with the sponge E110 oxidized at 1000 C (see Fig. 4.25).

It is obvious that this specific behavior of the sponge type zirconium-niobium binary alloys in the temperature range 900–1000 C is a function of the behavior of minor alloying elements (impurity elements) in this temperature range. The clarification of the physical nature in these processes is the task for future investigations.

Moreover, the extension of experimental data base, which will be obtained due to future investigations will allow to develop the practical approach to the assessment of the safety criteria for this temperature range because two opposite effects must be taken into account:

1. Decrease of the oxidation rate.

- Increase of the brittle α -Zr(O) layer thickness and, consequently, the reduction of the ductile prior β -layer after comparing as a function of time (taking into account the phenomena associated with p.1).

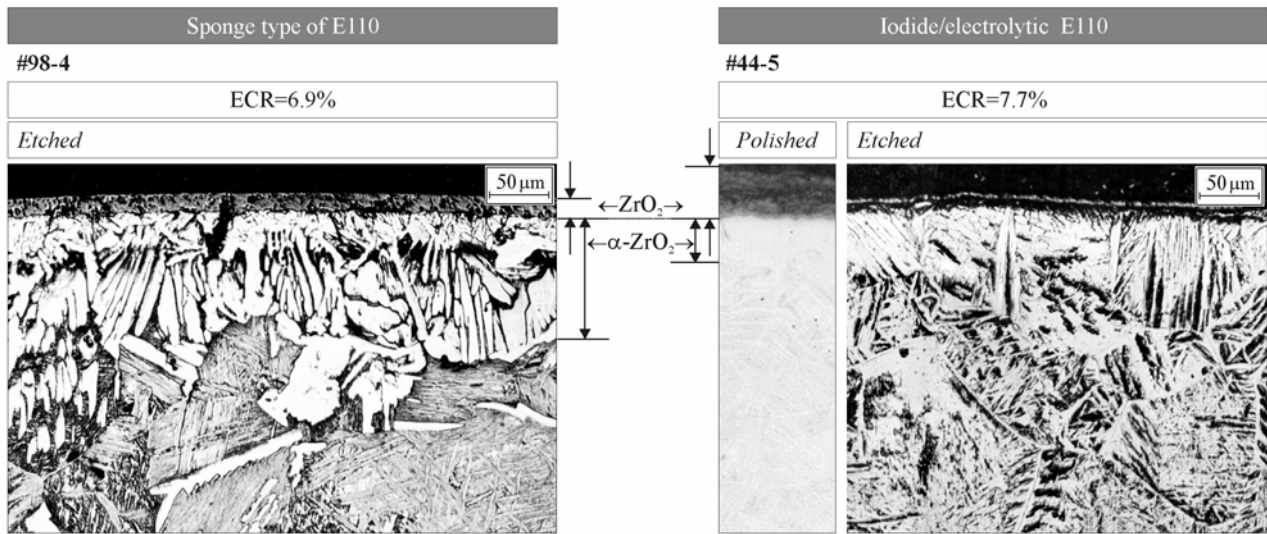


Fig. 4.24. The difference in the thicknesses of ZrO_2 and α -Zr(O) layers in the E110 cladding of sponge and iodide/electrolytic types at the oxidation at 1000 C

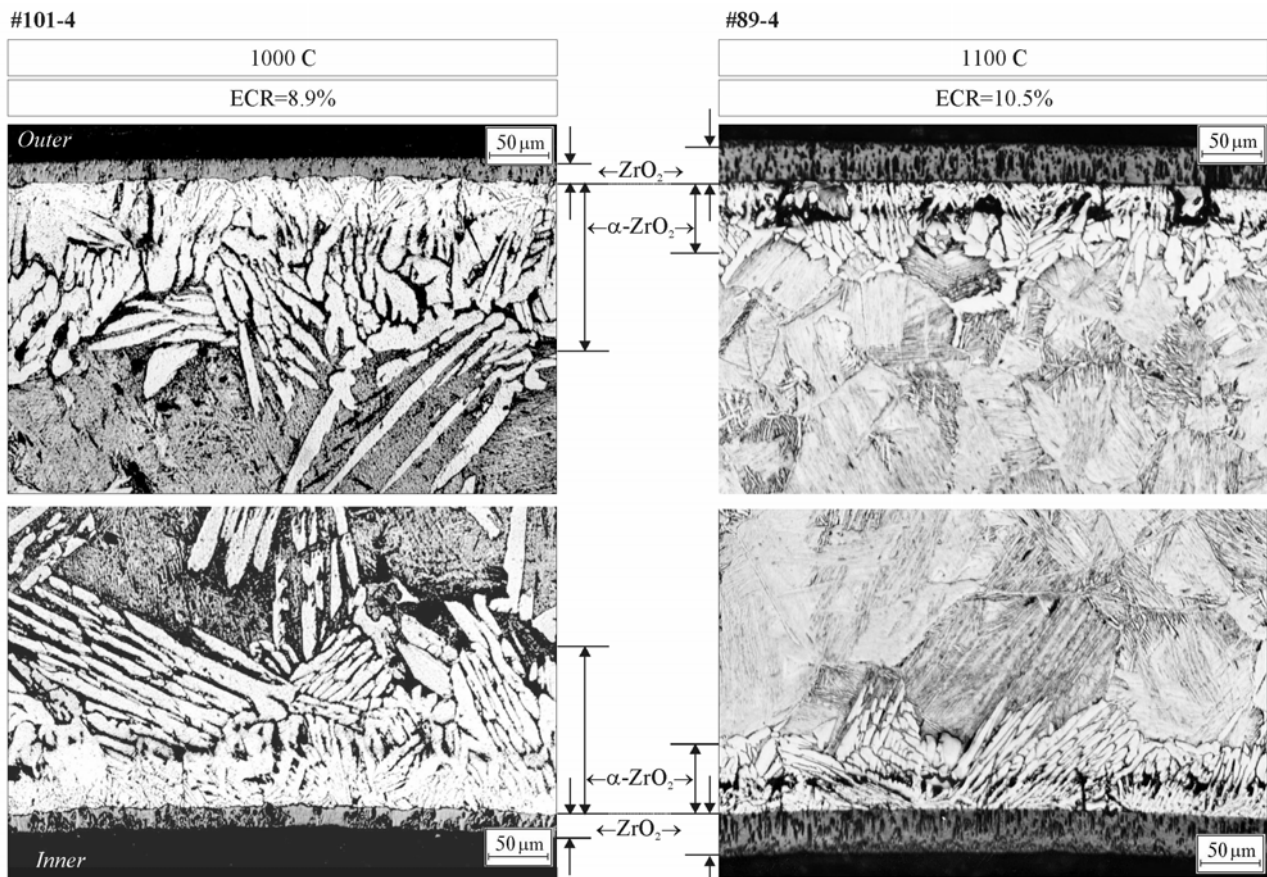


Fig. 4.25. The difference in the formation of oxide and α -Zr(O) layers in the E110 cladding of sponge type at 1000 and 1100 C

The preliminary recommendations concerning this issue will be presented in the Summary of the report.

REFERENCES FOR SECTION 4

- [1] Brachet J., Pelchat J., Hamon D., Maury R., Jaques P., Mardon J. "Mechanical Behavior at Room Temperature and Metallurgical Study of Low-Tin Zry-4 and M5™ (Zr-NbO) Alloys after Oxidation at 1100°C and Quenching", *Proc. of IAEA Technical Committee Meeting on "Fuel Behavior under Transient and LOCA Conditions"*, Halden, Norway, September 10-14, 2001.
- [2] Mardon J., Frichet A., LeBourhis A. "Behavior of M5™ Alloy under Normal and Accident Conditions", *Proc. of Top Fuel-2001 Meet.*, Stockholm, May 27-30, 2001.
- [3] Ageenkova L., Braslavsky G., Kishenevsky V., Nikulina A., Tararaeva E., Shebalov P., Zaimovsky A. "Structural and Phase Transformation in Zr-Nb Binary Alloys and their Relation to Properties", *Proc. of Conference on Reactor Physical Metallurgy*, v.6, 29.5–1.6 1978, Alushta, Russia (rus).
- [4] Zaimovsky A., Nikulina A., Reshetnikov N. "Zirconium alloys in the Nuclear Industry", Moscow, Energoizdat, 1981 (rus).
- [5] Shebalov P., Peregud M., Nikulina A., Bibilashvili Yu., Lositski A., Kuz'menko N., Belov V., Novoselov A. "E110 Alloy Cladding Tube Properties and their Interrelation with Alloy Structure Phase Conditions and Impurity Content", *Proc. of Zirconium in the Nuclear Industry: Twelfth International Symposium*, ASTM STP 1354 (p. 545), 2000.
- [6] Reshetnikov F., Bibilashvili Yu., Golovnin I. "The Development, Manufacture and Operation of Fuel Rods of Nuclear Power Reactors", Moscow, Energoatomizdat (rus), 1995.
- [7] Mardon J., Charquet D., Senevat J. "Influence of Composition and Fabrication Process on Out-of-Pile and In-Pile Properties of M5 alloy", *Proc. of Zirconium in the Nuclear Industry: Twelfth International Symposium*, ASTM STP 1354 (p. 505), 2000.
- [8] Jeong Y., Kim H., Kim T., Jung Y. "Effect of Nb-concentration, Precipitate, and Beta Phase on Corrosion and Oxide Characteristics of Zr-xNb Binary Alloys", *Zirconium in the Nuclear Industry: Thirteenth International Symposium* (poster paper).
- [9] Jeong Y., Kim H., Kim T. "Effect of β -phase, Precipitate, and Nb-concentration in Matrix on Corrosion and Oxide Characteristics of Zr-xNb Alloys", *Journal of Nuclear Materials*, v.317, 2003.
- [10] Kalin B. "The Investigation of Structure of Zirconium Alloys at the Alloy Modifications with the Use of Power and Radiation Attacks", *Proc. of Nuclear Power on the Threshold of the XXI Century Conference*, 8–10 June 2000, Electrostal, Russia (rus).
- [11] Kalin B., Osipov V., Volkov N., Gurovich B., Atalikova I., Menaykin S. "The oxide morphology in the zirconium alloys after its modification by the ion alloying technic", *Proc. of the 5th Conference on the Reactor Physical Metallurgy*, Dimitrovgrad, Russia, 8–12 September 1997.
- [12] Chung H.M. "The Effects of Aliovalent Elements on Nodular Oxidation of Zr-based Alloys", *Proc. of the 2003 Nuclear Safety Research Conference*, Washington DC, October 20-22, 2003, NUREG/CP-0185, 2004.
- [13] M. Billone, Y. Yan and T. Burtseva. "Post-Quench Ductility of Advance Alloy Cladding", *NSRC Conference*, Washington DC, USA, October 20–22, 2004.
- [14] Lunde L., Videm K. "Effect of Material and Environmental Variables on Localized Corrosion of zirconium Alloys", *Proc. of Zirconium in the Nuclear Industry Conference*, ASTM STP 681, 1979.
- [15] Wagner C., *Naturwissenschaften*, 31(1943), 265.
- [16] Vrtilkova V., Valach M., Molin L. "Oxidizing and Hydrating Properties of Zr-1%Nb Cladding Material in Comparison with Zircalloys", *Proc. of IAEA Technical Committee Meeting on "Influence of Water Chemistry on Fuel Cladding Behavior"*, Rez (Czech Republic), October 4-8, 1993.
- [17] Takeda K., Anada H. "Mechanism of Corrosion Rate Degradation Due to Tin", *Proc. of Twelfth International Symposium "Zirconium in the Nuclear Industry"*, ASTM STM 1354 (p. 592), 2000.
- [18] Mardon J.P., Waeckel N. "Behavior of M5™ Alloy under LOCA Conditions", *Proc. of Top Fuel-2003 meetings "Nuclear Fuel for Today and Tomorrow Experience and Outlook"*, March 16-19, 2003, Wurzburg, Germany.

- [19] Charquet D. "Microstructure and Properties of Zirconium Alloys in the Absence of Irradiation", *Proc. of Twelfth International Symposium: Zirconium in the Nuclear Industry*, ASTM STP 1354.
- [20] Kakiuch K., Itagaki, Furuya T., Miyazaki A., Ishii Y., Suzuki S., Yamawaki M. "Effect of Iron for Hydrogen Absorption Properties of Zirconium Alloys", *Proc. of Top Fuel-2003 Meeting "Nuclear Fuel for Today and Tomorrow Experience and Outlook"*, March 16–19, 2003, Wurzburg, Germany.
- [21] Murai T., Isobe T., Takizawa Y., Mae Y. "Fundamental Study on the Corrosion Mechanism of Zr-0.2Fe, Zr-0.2Cr, and Zr-0.1Fe-0.1Cr Alloys", *Proc. of Twelfth International Symposium: Zirconium in the Nuclear Industry*, ASTM STP 1354.
- [22] Warr B.D., Perovic V., Lin Y.P., Wallace A.C. "Role of Microchemistry and Microstructure on Variability in Corrosion and Deuterium Uptake of Zr-2.5Nb Pressure Tube Material", *Proc. of Zirconium in the Nuclear Industry: Thirteenth International Symposium*, ASTM STP 1423.
- [23] Ploc R.A. "The Effect of Minor Alloying Elements on Oxidation and Hydrogen Pickup in Zr-2.5Nb", *Proc. of Zirconium in the Nuclear Industry: Thirteenth International Symposium*, ASTM STP 1423.
- [24] Meyer R. "NRC Activities Related to High Burnup New Cladding Types, and Mixed-Oxide Fuel", *Proc. of an International Topical Meeting on Light-Water-Reactor-Fuel-Performance*, April 10-13, 2000, Park City, Utah, USA, (v.1).
- [25] Nikulina A.V., Andreeva-Andrievskaya L.N., Shishov V.N., Pimenov Yu.V. "Influence of Chemical Composition of Nb Containing Zr Alloy Cladding Tubes on Embrittlement under Conditions Simulating Design Basis LOCA", *Fourteenth International Symposium on Zirconium in the Nuclear Industry*, June 13-17, 2004.
- [26] Motta A., Ervin K., Delaire O., Birtcher R. Chu Y., Maser J., Mancini D., Lai B. "Synchrotron Radiation Study of Second-Phase Particles and Alloying Elements in Zirconium Alloys", *Proc. of Zirconium in the Nuclear Industry: Thirteenth International Symposium*, ASTM STP 1423.
- [27] D.Gilbon et.al. "Irradiation Creep and Growth Behavior, and Microstructural Evolution of Advanced Zr-Base Alloys", *Proc. of Zirconium in the Nuclear Industry: Twelfth International Symposium*, ASTM-STP 1354.

5. SUMMARY

During 2001–2004, research was performed to develop test data on the embrittlement of niobium-bearing cladding of the VVER type under LOCA relevant conditions. The program variability is shown in Fig. 5.1.

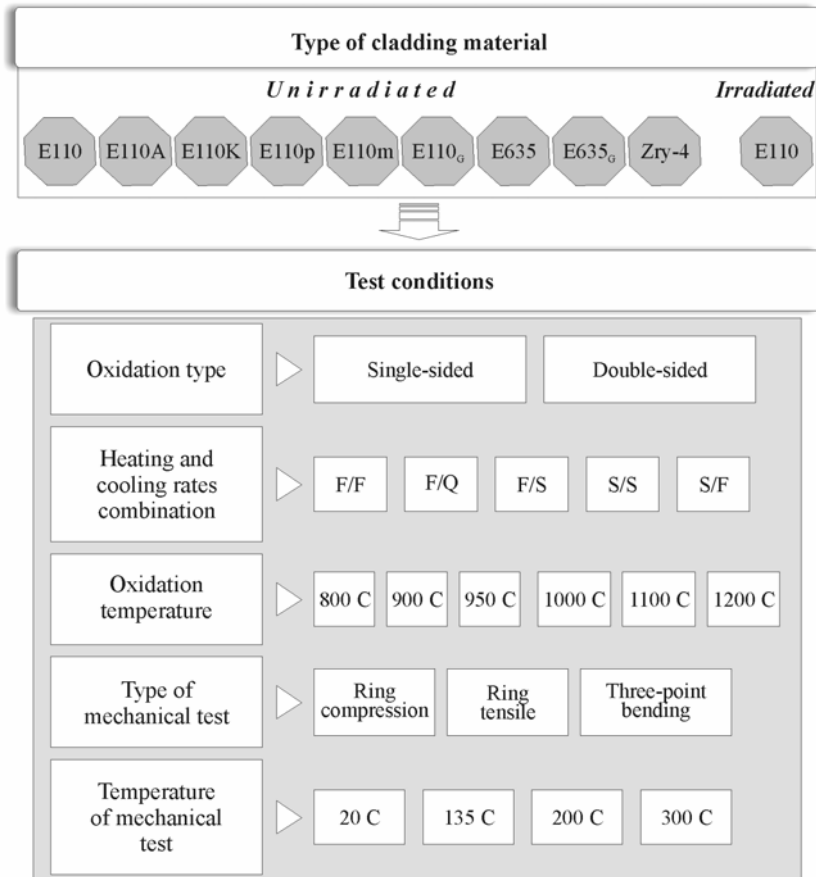


Fig. 5.1. Outline of the research program

The results of previous investigations suggested the following list of tasks for the program first part:

- procedure development and validation to determine the zero ductility threshold;
- determination of the zero ductility threshold sensitivity to transient conditions of the LOCA scenario (variations of heating and cooling rates during the oxidation);
- development of the experimental data base characterizing the oxidation kinetics in the temperature range 800–1200 C and zero ductility threshold of Zr-1%Nb cladding of the VVER type (the E110 alloy);
- comparative analysis of the oxidation and mechanical behavior of Zircaloy-4, E110 (Zr-1%Nb) and other niobium-bearing claddings.

5.1. Major findings of the program first part

5.1.1. Methodological aspects of mechanical tests

Consideration of the safety problem associated with the prevention of a fuel rod fragmentation caused by the embrittlement of a fuel rod cladding during the high temperature oxidation under LOCA conditions has shown that two general approaches could be used to estimate the appropriate phenomena:

1. An approach based on the determination of the oxidized cladding fragmentation threshold.
2. An approach based on the determination of the cladding material embrittlement threshold.

From the formal point of view, the approach based on the determination of the cladding fragmentation threshold is preferable because the loss of resistance to the combination of accident loads is directly estimated in this case. Impact tests and thermal-shock tests are typical examples of this approach practical implementation. However, to use results of these tests for the safety analysis, the representativity of test conditions should be demonstrated in comparison with the combination of loads under real accident conditions. But it is known that real loads on the embrittled cladding during the accident cannot be estimated at present with sufficient accuracy. Besides, the whole previous experience shows that the cladding fragmentation threshold cannot be less than the cladding embrittlement threshold. Moreover, taking into account that embrittlement threshold is the basic material property this threshold depends only weakly on the type of mechanical tests. Therefore, the conservative approach was used to estimate the Zr-1%Nb (E110) embrittlement condition.

Special scoping tests were performed to develop a comparative data base characterizing the E110 zero ductility threshold using the following types of mechanical tests:

- ring tensile;
- ring compression;
- three-point bending.

In accordance with the obtained data, the ring tensile and ring compression tests led to the same zero ductility threshold of the oxidized cladding. Three-point bending tests overestimated this threshold in comparison with ring compression and ring tensile tests.

Taking into account these results and the fact that ring compression tests were used for the validation of the current safety criteria for the zircaloy cladding, this type of mechanical tests was chosen for the research. Some characterization of the oxidized cladding behavior under these test conditions are presented in Fig. 5.2.

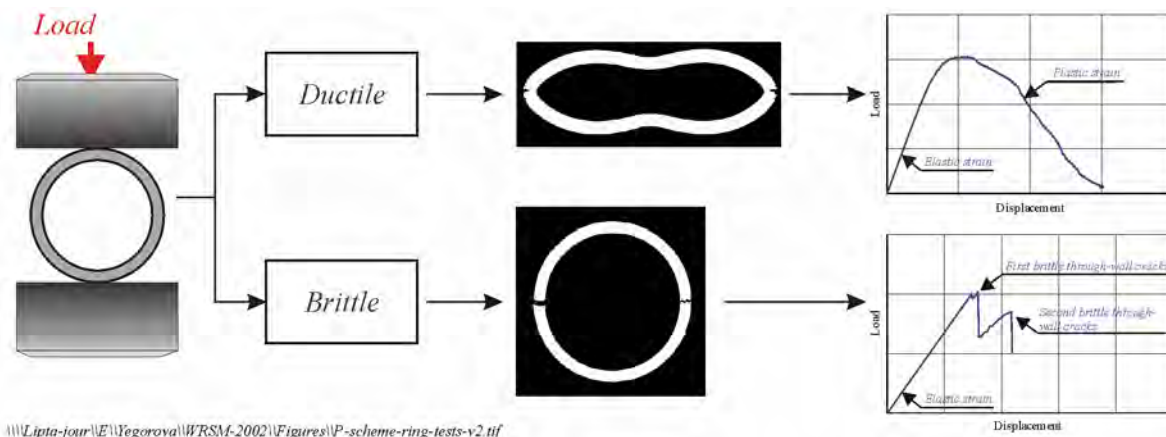


Fig. 5.2. The schematics of ring compression tests

The additional analysis has shown that in spite of the fact that ring compression tests have the thirty year history many issues concerning the procedure of these tests still remain to be solved. Thus, the previous popular approach to the processing of ring compression test results based on the determination of relative displacement at failure (the sum of “elastic” and “plastic” displacement divided by the cladding outer diameter) did not allow to estimate the zero ductility threshold in the explicit form (see Fig. 5.3). Besides, the length of ring samples varied in the range 6–30 mm and the procedure for the fracture determination on the basis of load-displacement diagrams was not validated.

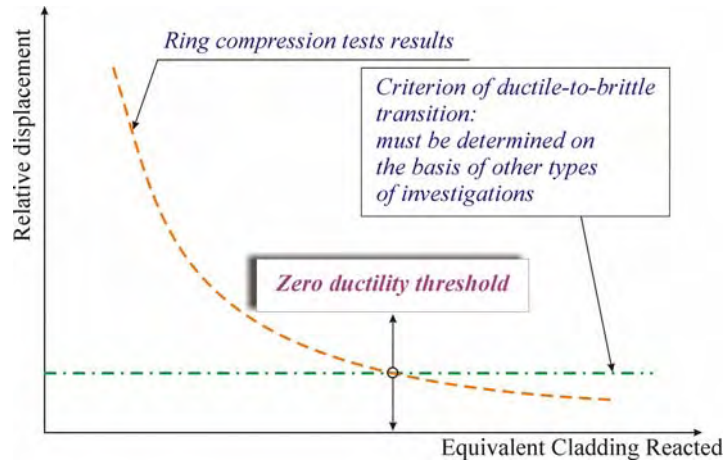


Fig. 5.3. The schematic of previous approach to the determination of zero ductility threshold

Using results of a special experimental subprogram the following outcomes were obtained:

- an approach to the determination of the zero ductility threshold on the basis of processing of load-displacement diagrams has been selected;
- major provisions of this approach are based on the direct connection between the ductility margin and plastic strain value. To estimate the plastic strain, the parameter named the residual ductility at failure has been defined (see Fig. 5.4). When the residual ductility at failure tends to zero the ductile-to-brittle transition (zero ductility threshold) occurs in the oxidized cladding;
- it is obvious that the selected method allows to obtain the macroscopic estimation of the zero ductility threshold only. But the fractography examinations performed with several samples confirm that the macroscopic and microscopic experimental data are in a good agreement;
- to determine the fracture condition (the first through-wall crack) at the processing of load-displacement diagrams, a special reference data base has been developed;
- the ring compression tests performed with rings of different length have shown that the residual ductility at failure does not depend on ring length in the range 8–25 mm for specially prepared ring samples. This special preparation consists in the elimination of the oxidized sample end parts (5 mm approximately) before the ring compression test. In other case the zero ductility threshold may be underestimated significantly.

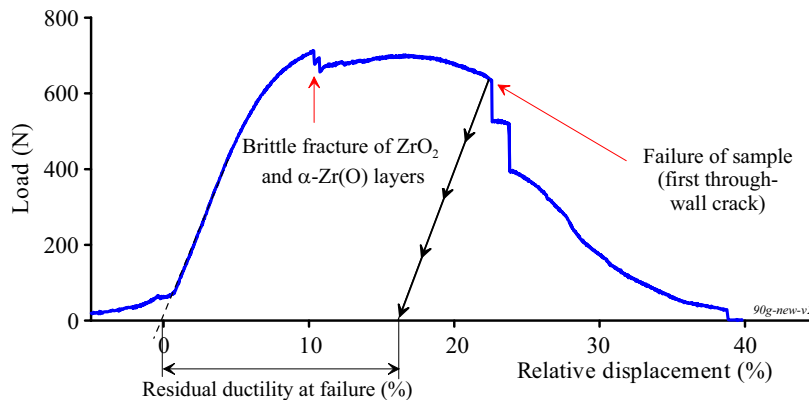


Fig. 5.4. The interpretation of ring compression test results on the basis of the load-displacement diagram

5.1.2. Methodological aspects of oxidation tests

A special scope of analytical and experimental work was performed to validate the following parameters of the oxidation facility:

- the uniformity of the temperature distribution along the long cladding sample (100 mm);
- the representativity of the cladding temperature measurements;
- the absence of steam starvation conditions around the cladding sample.

Taking into account the likely spallation and loss of zirconium dioxide on the oxidation of the E110 cladding a special method for the weight gain measurement was developed, verified and implemented.

To determine the zero ductility threshold sensitivity to such parameters of the oxidation scenario as heating and cooling rates, special scoping tests were performed. The major parameters of these tests are shown in Fig. 5.5.

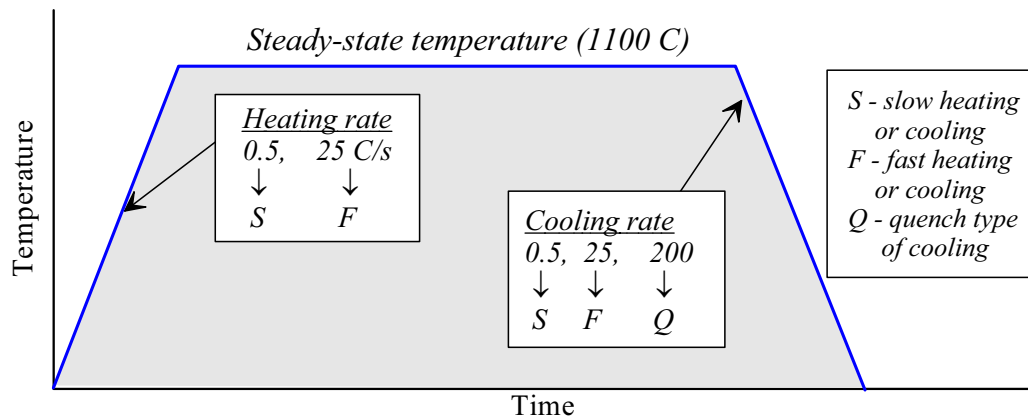


Fig. 5.5. The variability of oxidation tests with different heating and cooling rates

Numerous oxidation tests were performed with five combinations of heating and cooling rates: S(0.5 C/s)/F(25 C/s), S(0.5 C/s)/S(0.5 C/s), F(25 C/s)/S(0.5 C/s), F(25 C/s)/F(25 C/s), F(25 C/s)/ Q(200 C/s) where S means slow, F means fast, and Q means quench. Test results have shown that:

- the specific features of the E110 oxidation behavior are present at any combination of heating and cooling rates;
- the most pronounced negative phenomena accompanying the E110 high temperature oxidation are observed at slow heating rate (0.5 C/s).

Nevertheless, the comparative analysis of zero ductility thresholds obtained for these five combinations of heating and cooling rates allowed to make the following important conclusions:

- the zero ductility threshold has a low sensitivity to the combination of heating and cooling rates;
- the zero ductility threshold of the oxidized cladding at cooling with 25 C/s (F) and 200 C/s (Q) is practically the same.

These test results allowed to perform all subsequent investigations using the F/F (25 C/s/25 C/s) combination of heating and cooling rates.

In the frame of this research program, almost all oxidation tests were performed under double-sided oxidation conditions. But to widen the data base for the comparative analysis, a special subprogram was carried out under single-sided oxidation conditions. The obtained results have shown that the zero ductility threshold of the E110 is increased from about 8% ECR for double-sided oxidation to about 11% for single-sided oxidation.

The general verification of experimental procedures developed for this program was the final stage of methodological work. The verification was performed in reference tests with Zry-4 cladding. After that, the obtained results were compared with the numerous published data on this alloy. Results of this comparison

have shown that the set of experimental procedures developed to determine the zero ductility threshold of Zr-1%Nb (E110) cladding do not introduce large systematic errors.

5.1.3. The embrittlement behavior of Zr-1%Nb (E110) cladding

This stage of the research program was performed with the use of commercial as-received E110 cladding tubes. The double-sided oxidation tests were carried out with these tubes in the temperature range 800–1200 C at F/F (25 C/s/25 C/s) and F/Q (25 C/s/200 C/s) combinations of heating and cooling rates. The embrittlement characteristics of oxidized claddings were determined using the ring compression tests at 20 C. For reference, mechanical tests were also performed at 135, 200, 300 C. This data base was supplemented with results of reference tests with the Zry-4 cladding, which was oxidized at 1100 C and tested at 20 and 135 C.

The visual observations of oxidized E110 claddings have shown that this material is characterized by the initiation of the breakaway oxidation and earlier embrittlement in comparison with the Zry-4 cladding. So, some experimental data obtained at 1100 C and presented in Fig. 5.6 allow to make the following general conclusions (all ECR values are as measured):

- the uniform oxidation mode characterizes the E110 oxidation at low ECR (0–6.5% in this case). This oxidation mode leads to the formation of a black protective oxide on the cladding surface;
- the breakaway oxidation mode occurs with the increase of the ECR up to 10.5% (in presented case). This oxidation mode is accompanied by oxide spallation;
- the reference Zry-4 cladding surface oxidized at 11.3% ECR is covered with the black lustrous oxide. This fact confirms that the breakaway oxidation condition was not achieved in the Zry-4 cladding material.

Cladding material	As-measured ECR (%)	Appearance of 100 mm oxidized samples
E110	6.5	
	10.5	
Zry-4	11.3	

Fig. 5.6. The appearance of the E110 and Zry-4 claddings (1100 C) as a function of the ECR

The reassessment of previous investigations allow to establish that the cladding embrittlement after the breakaway oxidation is a sum of two processes:

1. The oxygen induced embrittlement caused by the formation of ZrO_2 and α -Zr(O) brittle layers, the decrease of the prior β -phase thickness and the increase of oxygen concentration in the prior β -phase.
2. The hydrogen induced embrittlement caused by the hydrogen absorption in the prior β -phase and hydriding of the cladding material.

Taking into account these considerations, the data base characterizing the residual ductility of the oxidized E110 cladding as a function of the ECR was supplemented with the numerous measurements of hydrogen concentration in the oxidized claddings (see Fig. 5.7).

The major outcomes of results obtained at 1100 C are the following:

- the E110 oxidized cladding has a very high ductility margin and low hydrogen content in the cladding material at the ECR up to 7.0%;

- a sharp decrease of the E110 ductility occurs in the range of 7–8% ECR. This process corresponds to a sharp increase of hydrogen content in the prior β -phase of the E110 oxidized cladding;
- the E110 zero ductility threshold is achieved at 8.3% ECR (as-measured) with 300–400 ppm of hydrogen content;
- the Zry-4 reference cladding has demonstrated sufficient margin of residual ductility and very low hydrogen content at 11.3% ECR.

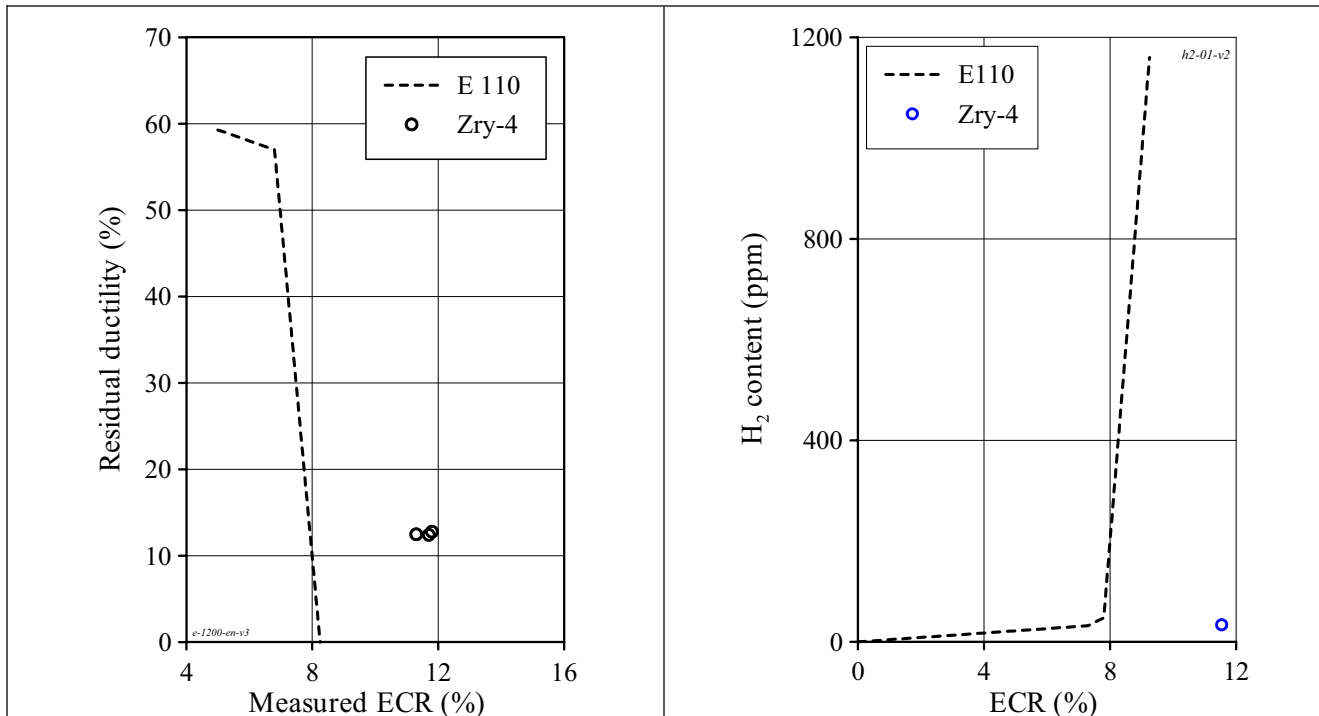


Fig. 5.7. The E110 residual ductility and hydrogen concentration as a function of the ECR after the double-sided oxidation at 1100 C and F/F, F/Q combinations of heating and cooling rates

To understand and to interpret the obtained results, special post-test examinations of metallographic samples were performed on the basis of the optical microscopy, SEM investigations, Auger spectroscopy, fractography, and microhardness measurements. The analysis of these results with the support of data obtained during previous investigations allowed to make the following important observations and comments:

- the cracking and spallation of the ZrO_2 layer observed on the E110 cladding at the ECR higher than 7% provide hydrogen penetration into the oxide metal interface;
- the cracking and spallation of the ZrO_2 layer is the result of transition from the understoichiometric protective tetragonal oxide to the stoichiometric porous monoclinic oxide;
- this tetragonal-monoclinic phase transition is a function of temperature and volume stresses;
- the stabilization of the protective tetragonal oxide prevents the hydrogen penetration into the cladding material;
- most impurities in ZrO_2 that oxidize slower than Zr will stabilize the tetragonal oxide. It appears that a minor concentration of such elements as Sn, Fe, Cr in the zirconium dioxide allows to achieve this effect. This observation is in a good agreement with the Zry-4 alloying composition and oxidation behavior;
- but the presence of some other precipitates leads to the formation of heterogeneous ZrO_2 characterized by high volume stresses and the tendency towards early tetragonal-monoclinic transformation. It is obvious that ZrO_2 on the E110 cladding surface contains this type of precipitates.

The analysis of the wavelength dispersive x-ray (WDX) dot maps and electron probe microanalyzer (EPMA) results obtained in the frame of this work has shown that the redistribution of niobium in the α -Zr(O) layer is observed in the Zr-1%Nb oxidized cladding. This process is characterized by the formation of radially oriented Nb-enriched and Nb-depleted areas. This phenomenon may facilitate the development of the heterogeneous oxide ($\text{ZrO}_2(\text{Nb}_2\text{O}_5)$) with the tendency towards spallation. Besides, taking into account that niobium stabilizes the β -Zr phase, the transformation of niobium enriched areas into the α -Zr(O) phase occurs at a higher oxygen concentration than in the areas with the lower niobium concentration. This effect is responsible for the irregular boundary front between α -Zr(O) and prior β -phase in these alloys.

In spite of the fact that the E110 oxidation rate is somewhat less than that in the Zry-4, the E110 α -Zr(O) thickness is larger due to the difference in the allotropic transition temperature of the α -Zr(O) phase in the E110 alloy produced at the higher oxygen concentration in the β -phase. This fact and the irregular α -Zr(O)/ β -phase boundary lead to the reduction in the effective prior β -phase thickness and to the increase of oxygen concentration in the prior β -phase. The tendency towards the uniform oxygen distribution across the prior β -phase does not improve the ductility margin also. But the analysis of the microhardness measurements has shown that the revealed differences in the embrittlement behavior of the E110 and Zry-4 claddings cannot be explained by the differences in the oxygen concentration in the β -phase because the E110 cladding with the high ductility margin and E110 cladding on the zero ductility threshold are characterized by similar microhardness values. This result confirms that the hydrogen absorption by the E110 cladding is the key factor determining the E110 embrittlement behavior. The hydrogen diffuses in the prior β -phase along radially oriented α -Zr(O) grains, the Nb-enriched β -phase lines in the α -Zr(O) are the channels for the hydrogen penetration also. Taking into account that the hydrogen solubility in the zirconium matrix is very sensitive to the temperature and, besides, the ductility of solid hydrides is strongly dependent on temperature, the mechanical behavior of the E110 oxidized cladding was compared at 20 C and 135 C (the coolant saturation temperature at the end of the LOCA reflood mode). The obtained results have shown that:

- in the case when the whole absorbed hydrogen inside the zirconium matrix is in solid solution at 20 C (<100 ppm), the E110 has very high ductility at 20 C. Therefore the increase of ductility margin does not occur in the range 20–135 C;
- the critical value of hydrogen content associated with the E110 zero ductility threshold is increased from 400 ppm at 20 C up to 900 ppm at 135 C. This effect is most likely associated with the increase of hydride ductility;
- the embrittled sample with hydrogen content higher than 1000 ppm is insensitive to the temperature in this range.

Several ring compression and ring tensile tests performed at the temperature 200–300 C have shown that the cladding ductility is sharply increased in the temperature range 20–200 C with any hydrogen content (1500 ppm is the maximum value). The temperature increase up to 300 C does not change the ductility margin in general.

Therefore, the results of these investigations allowed to conclude that:

- the Zry-4 embrittlement is caused by the oxygen absorption in the prior β -phase and by the reduction in prior β -phase thickness;
- the E110 embrittlement is a function of two processes: oxygen embrittlement and hydrogen embrittlement accompanied by the reduction in the prior β -phase thickness.

To estimate the representativity of obtained results for other oxidation temperatures, the additional oxidation tests were performed in the range 800–1200 C. This stage of investigations has shown that:

- the most pronounced effects of the breakaway oxidation were observed at the temperatures 950–1000 C (see Fig. 5.8). The zero ductility threshold in this temperature range is a little lower than that at 1100 C (7.5% ECR at 1000 C);
- in spite of the presence of breakaway effects at the temperature 800 C, the zero ductility threshold is increased at that temperature to more than 12% ECR. This conclusion is confirmed by the low hydrogen content in the oxidized cladding. The critical hydrogen concentration (about 400 ppm) is achieved at

about 12% ECR. A detailed analysis of appropriate physical processes is a task for the future research but preliminary it should be noted that this improved behavior of the E110 cladding can be associated with the two phase compositions of the zirconium matrix (α and β -phases, in this case, the concentration of β -phase is relatively low at this temperature), a very low thickness of α -Zr(O) at this temperature, and some other phenomena considered in the report;

- as for the temperature 1200 C, the zero ductility threshold of the E110 cladding is most likely not better than that at 1100 C in spite of the tendency towards the decrease of hydrogen absorption rate.

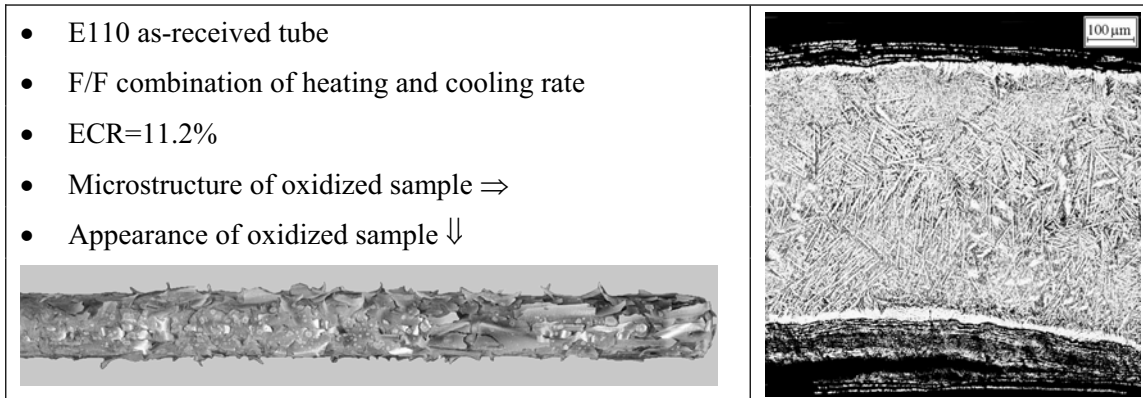


Fig. 5.8. Demonstration of the E110 breakaway oxidation effects at 950 C

To determine the sensitivity of the embrittlement behavior of niobium-bearing claddings to such alloying components as Sn and Fe, special investigations were performed with the E635 cladding (Zr-1%Nb-1.2%Sn-0.35%Fe). The analysis of obtained results showed that the visual appearance of E635 oxidized claddings was better than that of E110 claddings but in spite of this fact, the zero ductility threshold for these cladding materials was practically the same.

The last line of experimental investigations performed with the as-received E110 cladding tube was connected with the determination of the sensitivity of oxidation and mechanical behavior to the initial oxygen concentration in niobium-bearing alloys. The motivation to perform these studies was associated with the absence of a precise position on this issue in the current scientific publications and with the fact that the initial oxygen concentration in the tested E110 cladding was very low ($\sim 0.05\%$) in comparison with other alloys (including other niobium-bearing alloys). To develop the comparative data base, E110K as-received cladding tubes were tested. The initial oxygen concentration in this modification of the E110 alloy was about 0.11% by weight. The obtained test results allowed to establish that:

- the increase of oxygen concentration in the E110 alloy does not lead to suppression of the breakaway oxidation effect;
- the zero ductility threshold of the E110K cladding is not higher than that of the standard E110 cladding.

5.1.4. The embrittlement behavior of Zr-1%Nb (E110) cladding as a function of irradiation effects

Taking into account that the validation of high burnup fuel behavior under LOCA conditions is one of the urgent research problems, the preliminary stage of this type of investigations was performed in the frame of this work.

The irradiated E110 claddings refabricated from VVER high burnup fuel rods with burnup of about 50 MW d/kg U had the following characteristics before the oxidation tests:

- ZrO₂ thickness on the outer cladding surface was 5 μm ;
- ZrO₂ thickness on the inner cladding surface was 0 μm ;
- hydrogen content in the cladding material was 47 ppm.

The analysis of the appearance and metallographic examinations of the irradiated cladding oxidized in the temperature range 1000–1200 C at the F/F combination of heating and cooling rates allowed to reveal the following (see Fig. 5.9):

- the outer surface of oxidized irradiated claddings are covered with the black uniform oxide without the spallation effects up to 16% ECR based on the results of visual examinations;
- as for the inner surface, the tendency towards oxide spallation was noted at the 7.7% ECR and higher.

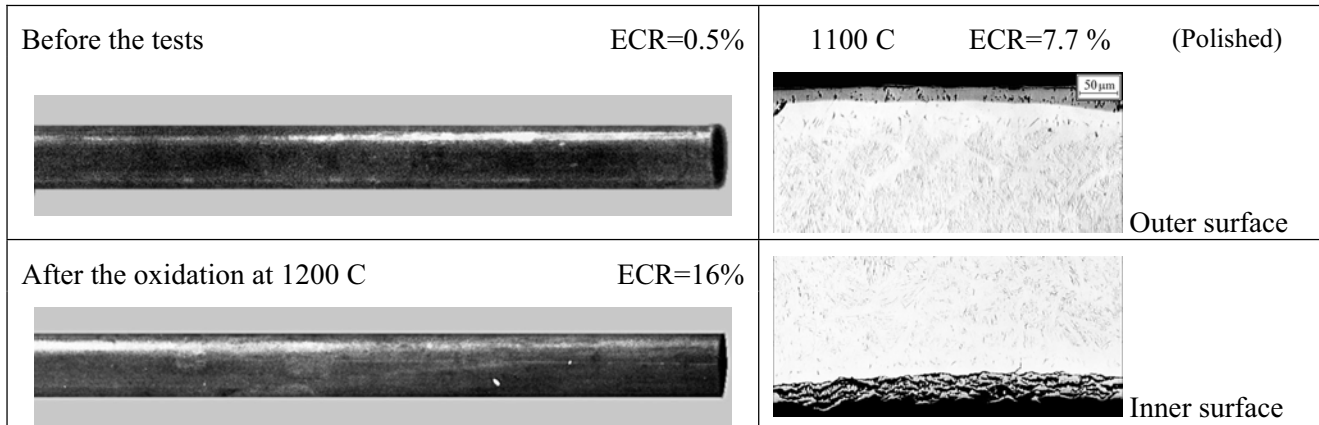


Fig. 5.9. The appearance and microstructure of the E110 irradiated claddings as a function of the ECR

The obtained data are in a good agreement with other Russian investigations performed in the MIR research reactor under LOCA conditions. The following general observations may be made on the basis of the whole scope of experimental data:

- the irradiation inhibits the breakaway oxidation tendency on the outer surface of the E110 cladding;
- the tendency towards oxide spallation is supplemented with the tendency towards an increase in oxidation rate (the oxide thickness increase) on the cladding inner surface. In accordance with these data, it may be assumed that the contamination of the cladding inner surface by fission products is responsible for these effects.

The consideration of the data base characterizing the residual ductility microhardness and hydrogen content in the oxidized irradiated cladding as a function of the ECR has shown that:

- in accordance with the postulated relationship between the oxygen concentration in the prior β -phase, microhardness, and the oxygen induced zero ductility threshold, this threshold corresponds to 8.3% ECR;
- the combination of the oxygen induced and hydrogen induced embrittlement of the E110 irradiated cladding leads to the reduction of the zero ductility threshold down to 6.5% ECR at the F/F combination of heating and cooling rates.

5.1.5. The oxidation kinetics and embrittlement behavior of the E110 cladding according to results of previous investigations in different laboratories

Earlier oxidation and ring compression tests with the E110 unirradiated cladding were performed in the following institutes:

- VNIINM, Russia [1];
- KFKI, Hungary [2, 3];
- NFI, Czech republic [4, 5];
- NC in Rossendorf, Germany [6, 7].

It should be noted that the comparative analysis of VNIINM test results was performed on the basis of data obtained at the end of 1980s of the past century. The recent VNIINM tests were not used because open VNIINM publications devoted to these issues did not contain the information in detail concerning test modes and test parameters.

The comparison of the E110 oxidation kinetics estimated according to the results of this work with oxidation kinetics obtained earlier has shown that the discrepancy between the RRC KI/RIAR, VNIINM, NFI, NC in Rossendorf results is low in the studied range of weight gains and temperatures (see Fig. 5.10). The KFKI data overestimates noticeably the E110 oxidation kinetics.

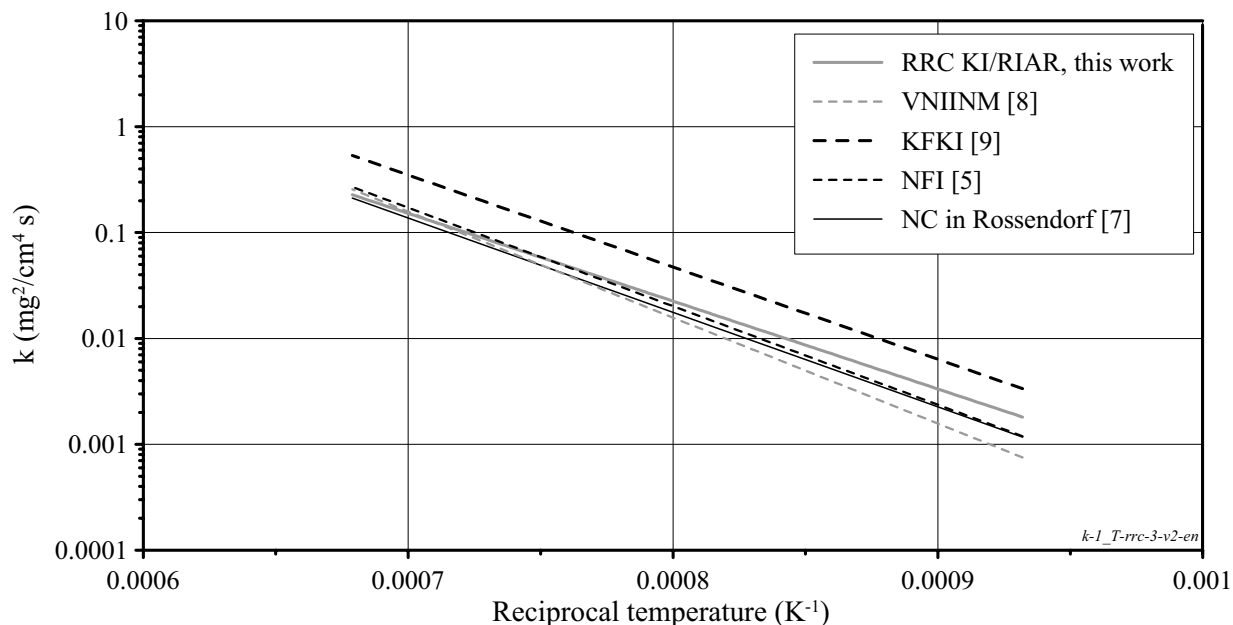


Fig. 5.10 The comparison of the E110 oxidation kinetics (1073–1473 K) in accordance with the data of different investigations

The comparison of the E110 and Zry-4 oxidation kinetics presented in Fig. 5.11 for the as-measured data and for the as-calculated data (with the use of Zry-4 conservative kinetics based on the Baker–Just correlation and E110 conservative kinetics developed in the VNIINM) allows to note the following:

- practically the same conservative kinetics is used for the safety analysis of the E110 and Zry-4 claddings;
- the as-measured E110 oxidation kinetics is noticeably less than that for the Zry-4 cladding.

The difference in the postulated safety criteria characterizes the E110 and Zry-4 fragmentation thresholds (18% and 17% respectively) and the difference in the E110 and Zry-4 oxidation kinetics leads to the following estimations of the as-measured oxidation corresponding to safety criteria at 1100 C:

- 11.5% ECR for E110;
- 13.5% ECR for Zry-4.

The preliminary data characterizing the oxidation kinetics of the E110 irradiated cladding showed that the oxidation rate of irradiated claddings was somewhat higher than that of unirradiated claddings at all oxidation temperatures (1000–1200 C). But taking into account the limited number of these tests, the investigations in this line should be continued in the future.

The analysis of comparative data characterizing the embrittlement behavior of the E110 unirradiated claddings allowed to note that all investigators revealed the tendency towards the breakaway oxidation of the E110 cladding accompanied by the hydrogen absorption and a sharp reduction in the residual ductility margin after the initiation of oxide spallation.

The consideration of the whole scope of the E110 test data obtained in the first part of this research led to the decision concerning the development of the program second stage to be devoted to the analysis of reasons for the E110 specific behavior in comparison with other niobium-bearing alloys.

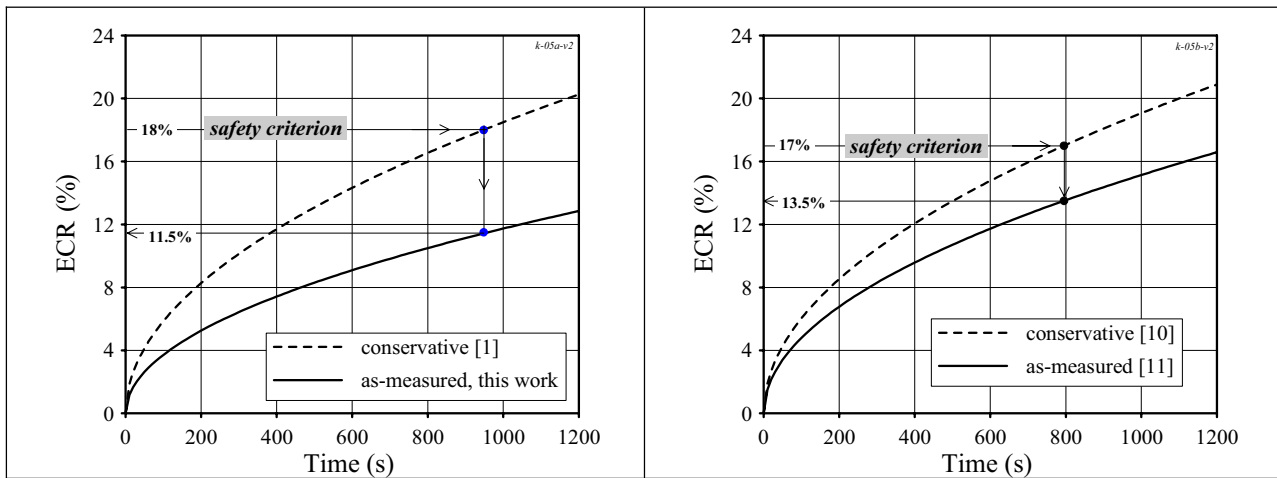


Fig. 5.11. The comparison of the E110 (on left) and Zry-4 (on right) conservative and as-measured kinetics at 1100 C

5.2. Major findings of the program second part

5.2.1. The concept of special investigations

The following general questions were formulated on the basis of the revealed general difference in the oxidation and embrittlement behavior of Zr-1%Nb (E110) and Zry-4 claddings:

Is the earlier breakaway initiation and the embrittlement caused by combined effects of oxygen and hydrogen uptake typical of the whole family of niobium-bearing alloys or does this phenomenon characterize the E110 alloy only?

The beginning of investigations to provide the answer to this question was devoted to the comparison of Zr-1%Nb (E110) embrittlement behavior with the behavior of other Zr-1%Nb claddings manufactured from the M5 alloy [12]. Published data with experimental results on the M5 cladding available by that time were used for this goal [13, 14]. The analysis of these M5 test results has shown that:

- the zero ductility threshold of the M5 cladding is higher than that of the E110 cladding;
- the breakaway oxidation is not observed in the investigated range of parameters;
- the M5 embrittlement is not accompanied by hydrogen uptake.

The analysis of possible reasons for the revealed difference between E110 and Zry-4 or M5 cladding behavior allowed to select the following phenomena for special studies:

- surface effects;
- bulk effects associated with the chemical composition of impurities in the cladding material;
- bulk effects associated with the cladding microstructure.

This part of the research program was closely coordinated with another experimental program being conducted at ANL at approximately the same time [15, 16]. The oxidation and mechanical tests were performed with M5, Zirlo, E110, and Zry-4 claddings in that program. The results of both programs allowed an extension of the comparative data base for observations and conclusions.

5.2.2. Surface effect studies

These studies were based on the following considerations:

- the corrosion resistance is a function of the cladding surface finish because the corrosion behavior depends on the surface chemistry (contaminations) and surface roughness;
- the sensitivity of the E110 cladding material to these phenomena should be estimated.

The urgency of this issue was determined by the fact that as-received E110 tubes used in the first part of the program were not subjected to surface finishing. The current E110 surface finishing procedure consisted of the final etching and anodizing of the cladding outer surface. To determine the sensitivity of the cladding embrittlement behavior to this procedure, the oxidation and mechanical tests with the etched and anodized E110A cladding were performed. The results of tests have shown that this surface finishing procedure does not allow to eliminate the earlier breakaway oxidation and to improve the embrittlement behavior of the E110 cladding.

Besides, one of the advanced methods for the surface finishing with the use of the outer surface grinding and inner surface jet etching was investigated also. But the conclusion was the same. Moreover, the tendency towards an increase in oxide thickness was revealed on the cladding inner etched surface. These results were in a good agreement with the ANL test data obtained with the E110 as-received tubes subjected to the special etching. The ANL tests showed that any etching led to the degradation of the cladding embrittlement behavior.

To eliminate the chemical contamination of the cladding surface caused by etching, special polished E110 samples were used for the next stage of the surface effect studies. The results of tests with this type of the cladding samples allowed to reveal the following (see Fig. 5.12):

- the visual indicators of the breakaway oxidation practically disappeared from polished parts of oxidized samples. The most pronounced effect was noted at 1000 C;
- the polished and unpolished parts of the oxidized cladding were characterized with quite a different hydrogen uptake;
- the residual ductility increased very significantly on the polished part of the oxidized cladding.

The same results have been obtained in similar investigations performed at ANL [15, 16].



Fig. 5.12. The appearance of the E110 polished and unpolished parts after the oxidation at 1000 C

Thus, the surface polishing allows to improve the oxidation and embrittlement behavior of the niobium-bearing cladding of the E110 type.

5.2.3. Bulk chemistry studies

Several investigations performed during last years have demonstrated that the oxidation behavior of niobium-bearing alloys is very sensitive not only to alloying components but also to the impurity composition. The analysis of the E110 problems in this context has shown that different methods are used to produce zirconium alloys for PWR and VVER claddings. In accordance with these methods, the sponge Zr is used to produce such alloys as Zry-4, M5, Zirlo and the mixture of iodide and electrolytic Zr is used for the fabrication of the E110 alloy.

It is obvious that the difference in the alloy production leads to the difference in the impurity compositions. This fact was accepted for the basis while developing a special subprogram devoted to the oxidation and ring compression tests with modified types of the E110 claddings (E110_G).

These modified types of the E110 claddings are the pilot samples produced by the Russian industry in accordance with the program of the sponge Zr introduction in the production of VVER claddings. The oxidation tests performed at 1100 C with different variants of the E110 sponge type claddings have demonstrated prac-

tically the same result. Macroscopic effects of the breakaway oxidation mode disappeared in the as-measured ECR range 10.5–18% (see Fig. 5.13).

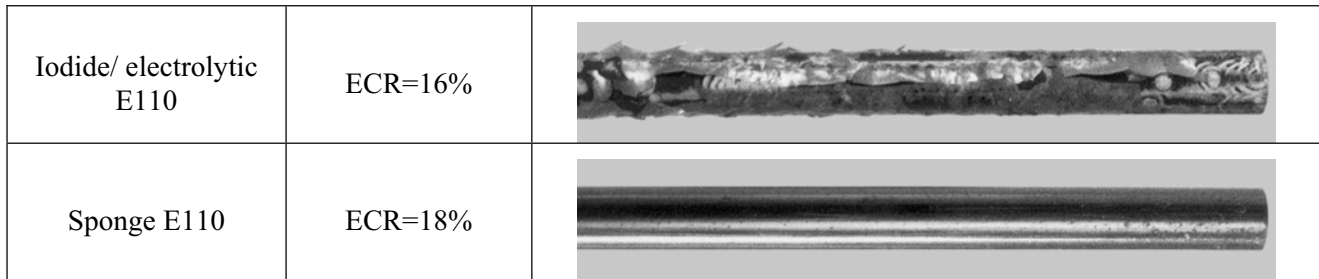


Fig. 5.13. The comparison of the iodide/electrolytic and sponge E110 cladding oxidation behavior at 1100 C

For oxidation at 1100 C, ring compression tests with oxidized claddings confirmed that the zero ductility threshold of the sponge E110 increased up to 19% ECR (as-measured) due to the low hydrogen uptake. The preliminary comparison of the embrittlement behavior of the sponge E110 and other alloys oxidized at 1100 C with the ANL published data on Zry-4, Zirlo, M5 test results [16] showed approximately the same zero ductility threshold.

Nevertheless, some difference was revealed in the hydrogen uptake for these claddings at 1100 C. Thus, Zry-4, Zirlo and M5 were characterized by the hydrogen content of 17–22 ppm at 19.1–21.1% ECR [16]. The E110 cladding kept the same hydrogen content (17 ppm) up to 16.7% ECR. But at 18% ECR, the hydrogen content increased up to 102 ppm. To determine the sensitivity of the sponge E110 to the oxidation temperature, special investigations were performed in the range 900–1200 C. These tests allowed to reveal several new phenomena.

For oxidation at 900 – 1000 C, major new phenomena were revealed and are associated with a sharp reduction of the sponge E110 oxidation rate in comparison with that of the iodide/electrolytic E110 (see Fig. 5.14), although at 1100 - 1200 C the oxidation kinetics of the sponge E110 and iodide/electrolytic E110 were similar with some tendency towards an increase of the oxidation rate in the sponge E110 claddings. The comparison of the sponge E110 with the other sponge type of Zr-1%Nb cladding (M5 alloy) performed with the use of French data [17] showed that oxidation kinetics of these alloys were the same at both temperatures.

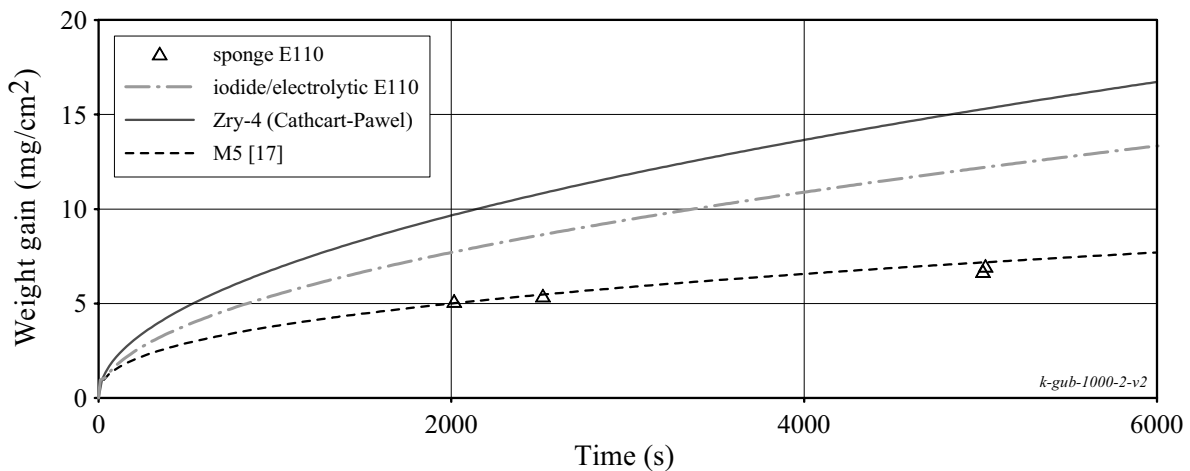


Fig. 5.14. The comparison of the Zry-4, sponge E110, iodide/electrolytic E110, M5 oxidation kinetics at 1000 C

The comparison of obtained data with the Zry-4 oxidation kinetics is presented as a function of temperature in Fig. 5.15.

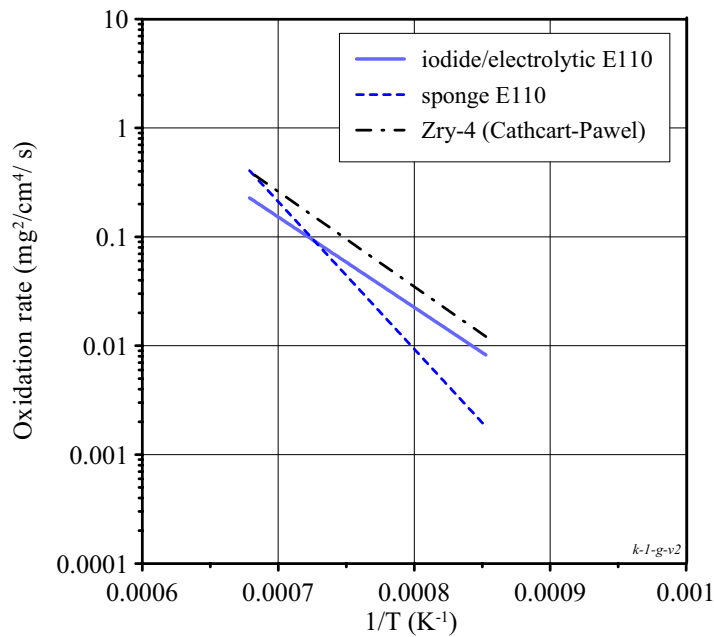


Fig. 5.15. The comparison of the Zry-4, sponge E110, iodide/electrolytic E110 oxidation rates in the temperature range of 900 - 1200 C

The data base obtained at 900 C and 1000 C to characterize the embrittlement behavior of the sponge E110 is not sufficient for the determination of the zero ductility threshold. Nevertheless, the analysis of test results allowed to make the following important conclusions:

- the ductility reduction as a function of ECR is caused by the oxygen induced mechanism at the low hydrogen uptake;
- the critical ECR associated with the zero ductility threshold at 900 C and 1000 C will be significantly lower than that at 1100 C, although the critical time will be significantly higher;
- a possible explanation of this phenomenon can be associated with the formation at 1000 C of a thicker α -Zr(O) layer in comparison with the α -Zr(O) layer formed at 1100 C or in comparison with the α -Zr(O) layer in the iodide/electrolytic E110 formed at 1000 C. This effect leads to the reduction of the effective thickness in the prior β -phase layer and to the increase of oxygen content in the metallic matrix;
- besides, the first indications of the breakaway oxidations (white spots on the cladding) appear at the $ECR \geq 8.5\%$, but this corresponds to a very long time.

It should be noted in the context of the revealed features that similar tendencies were noted in other Zr-1%Nb cladding alloys. Thus, a sharp reduction of M5 ductility was observed in the ECR range 11–12% (as-measured) in the ANL test data [15, 16]. Moreover, in accordance with results of French investigations, the breakaway phenomena accompanied by high hydrogen and nitrogen pickup were noted at 1000 C under the following conditions: the oxidation time was much higher than 1800 s but less than 135000 s [18]. It is of interest that the ANL data showed that Zirlo cladding did not demonstrate the tendency towards the earlier ductility reduction at 1000 C and it did not demonstrate a tendency of a sharp reduction in oxidation rate [15].

The next important data characterizing the sponge E110 behavior were obtained at the oxidation temperature 1200 C. The overview of appropriate results is as follows:

- in spite of the fact that visual indications of the breakaway oxidation were not observed up to the 23.3% ECR, a significant hydrogen uptake was revealed already at 8% ECR;
- the zero ductility threshold of the sponge E110 did not exceed the 8% ECR at 1200 C.

The comparison of these data with the ANL data [15, 16] characterizing the Zry-4, M5, Zirlo embrittlement behavior after the oxidation at 1200 C showed that:

- all tested alloys showed a tendency towards the reduction of the zero ductility threshold at this temperature. The Zry-4, Zirlo, M5 ductility reduction down to 5% (the residual ductility or offset hoop strain) occurred in the measured ECR range 8.2–10% ECR;
- but the Zry-4, Zirlo, M5 embrittlement was not accompanied by high hydrogen uptake. The hydrogen content in these claddings remained at the level ranging from 17–19 ppm up to 18.8–22.3% ECR.

The consideration of iodide/electrolytic and sponge E110 comparative data allows to assume that revealed general differences in the behavior of these cladding materials are a function of differences in the microchemical composition of these two modifications of the E110 alloy. To clarify the background of the problem, the results of previous investigations devoted to the relationship between the corrosion resistance of zirconium-based claddings and microchemical composition of the cladding alloy were reassessed. The major outcomes of this work were the following:

- the stabilization of zirconium dioxide tetragonal form led to the improvement of the cladding corrosion resistance;
- in this context, all impurities can be subdivided into the beneficial and deleterious impurities;
- in accordance with the physical theories and empirical data, the beneficial and deleterious impurities consisted of the following elements:
 - beneficial impurities: Fe, Cr, Ca, Mg, Y...
 - deleterious impurities: C, N, F, Cl, Si, Ti, Ta, V, Mn, Pt, Cu...
- there are contradictory points of view regarding such elements as Al, Ni, Mo. As for oxygen, the majority of investigators consider that this element is neutral with respect to corrosion resistance;
- the corrosion behavior was very sensitive to the concentration of such alloying elements as Nb and Sn. Moreover, each type of alloy had the optimal concentration of the alloying element at which the best corrosion resistance was provided;
- the main potential differences between the microchemical compositions of the iodide/electrolytic and sponge E110 alloy may be associated with the following:
 - the method of the electrolytic E110 production led to the risk of the alloy enrichment with such deleterious impurity as fluoride. Besides, the electrolytic E110 had a very high Hf content, the role of which was not quite understood with respect to the cladding corrosion behavior. The iodide Zr component of the alloy may be considered as neutral because this component had a very low content of both beneficial and deleterious impurities;
 - the method of the sponge E110 production facilitated the alloy enrichment with such beneficial impurities as Ca, Mg, Fe, Y.

Taking into account the results of this analysis, chemical compositions of iodide/electrolytic and sponge E110 alloys were compared. The comparison showed that reasonable differences in the impurity contents were revealed for two elements only:

- Fe: 86 ppm in the iodide/electrolytic E110 and 120–140 ppm in the sponge E110;
- Hf: 350 ppm in the iodide/electrolytic E110 and 90–420 ppm in the different modifications of the sponge E110.

It should be noted that it was impossible to compare directly the contents of many impurities of a low content in the alloy due to very low concentrations: the content was less than 10 ppm, 30 ppm, etc.

To determine the sensitivity of the E110 oxidation behavior, special tests were performed using the iodide/electrolytic E110 cladding with a low hafnium content (E110_{low Hf}, 90 ppm). These tests showed that the corrosion resistance was a function of hafnium content in the studied range of Hf variation (350 ppm in the iodide/electrolytic E110 and 90 ppm in the E110_{low Hf}).

The E110_{low Hf} cladding was characterized by the increase of the zero ductility margin from 8.3% ECR (standard E110) up to 12% ECR due to the significant delay in the breakaway initiation as a function of ECR. However, the fact cannot be ruled out that in this case the process of the E110 alloy purification from

hafnium might be accompanied by the change in the content of any other impurity because some modifications of the sponge E110 tested in the frame of this work constituted the mixture of sponge Zr, iodide Zr and recycled scrap with a high hafnium content but the corrosion resistance of these modifications was very high.

The next position of special investigations was associated with the determination of the sensitivity of the oxidation behavior of niobium-bearing alloys to the iron content:

- the oxidation and mechanical tests of the E635 cladding with a very high iron content in the cladding material (0.34–0.4% by weight) showed that the oxidation behavior and embrittlement threshold of iodide/electrolytic E635 was somewhat better than that for the iodide/electrolytic E110 but the sponge variant of E635 had practically the same embrittlement characteristics as iodide/electrolytic E635. And both versions of the E635 alloy had lower zero ductility thresholds (at 1100 C) than the sponge E110;
- the analysis of special investigations performed by the VNIINM [19] with the variation of iron content in the range 80–1400 ppm and the variation of such elements as O, C, Hf, Cr showed that:
 - in spite of the fact that the oxidation and mechanical response of seven types of the oxidized cladding (10% ECR) differentiated from the best (lustrous black oxide, low hydrogen content, reasonable margin of residual ductility) to the worst (breakaway effects, oxide spallation, high hydrogen content, low residual ductility), a direct association between the appropriate response and combinations of the chemical composition limited with such elements as Nb, Fe, C, Hf, Cr, O was not managed to be revealed. This fact undoubtedly indicated that the influence of other varied elements or some other parameters was not taken into account;
 - nevertheless, it should be noted that the best corrosion behavior of the tested cladding was obtained with an iron content of about 130–450 ppm and low hafnium content (~100 ppm) and a low carbon content. Very low (80 ppm) and very high (1400 ppm) iron contents were associated with the intermediate corrosion behavior but were also associated with very high carbon content (up to 200 ppm) in several samples.

Finally, the following general recommendations concerning the relationship between the microchemical composition and embrittlement behavior of niobium-bearing alloys can be given:

- the characterization of types of niobium-bearing alloys based on the current list of alloying elements should be reassessed;
- the status of some impurity elements must be changed and the definition of minor alloying elements should be added to the characterization of the cladding alloy;
- special investigations to determine the deleterious, beneficial and neutral impurities in the niobium-bearing alloys should be performed additionally.

5.2.4. Bulk microstructure studies

The last position of this stage of the research program was connected with the comparison of the microstructure parameters of different types of E110 cladding. To develop the data base for the comparison, TEM examinations of iodide/electrolytic E110 and sponge E110 cladding materials were performed.

In accordance with the results of analytical studies, the following comparative data were measured:

- phase conditions and phase composition;
- the grain size of zirconium in the cladding matrix;
- the parameters of the secondary phase precipitates being of importance for the corrosion resistance: the chemical composition, size, density, uniformity of distribution.

The choice of these comparative data was based on the results of inside and outside Russian investigations devoted the determination of the relationship between the corrosion behavior and cladding microstructure.

The results of TEM investigations showed that:

- iodide/electrolytic E110 and sponge E110 had a completely recrystallized microstructure ($\alpha+\beta$ -Nb);
- the average size of α -Zr grain in the matrix was similar for both types of E110 claddings (2.8 μm for iodide/electrolytic E110 and 3.2 μm for the sponge E110);
- the globular type of β -Nb precipitates uniformly distributed in the α -Zr matrix characterized both E110 modifications;
- the average size of the secondary β -Nb precipitates was practically the same in the iodide/electrolytic and sponge E110 (41–60 μm);
- the iodide/electrolytic E110 did not contain the intermetallic precipitates; the sponge E110 had the intermetallic precipitates of the $\text{Zr}(\text{Nb},\text{Fe})_2$ type, and the size of these precipitates was about 180 μm .

The comparative analysis of the iodide/electrolytic E110 and sponge E110 microstructures with the French published data on the M5 microstructure allowed to conclude the following:

- iodide/electrolytic E110 (E110_{low HF}), sponge E110 and M5 had practically the same parameters for the microstructure;
- the only distinction between the microstructure of iodide/electrolytic E110 and sponge types of Zr-1%Nb cladding (sponge E110, M5) was that the sponge Zr-1%Nb types of alloy had the iron-based precipitates in addition to the β -Nb precipitates.

5.2.5. Final Remarks

Taking into account the results of investigations devoted to the microstructure, microchemical and surface effects, the following general conclusions can be made:

- the current type of the E110 (Zr-1%Nb) cladding (standard iodide/electrolytic) has quite an optimal microstructure. The specific oxidation behavior of this cladding at high temperatures is not a function of the cladding microstructure;
- the performed research allowed to establish that the oxidation behavior and ductility margin of the E110 oxidized cladding are very sensitive to the cladding microchemical composition and surface finishing;
- the use of the sponge type of zirconium for the fabrication of cladding tubes provides a significant reduction of the cladding oxidation rate, especially in the temperature range of 900 – 1000 C, and an increase in the zero ductility threshold;
- additional improvement of the oxidation behavior and a significant increase of the residual ductility margin in the E110 oxidized cladding can be achieved by polishing of the outer and inner cladding surfaces.

REFERENCES FOR SECTION 5

- [1] Bibilashvili Yu.K., Sokolov N.B., Dranenko V.V., Kulikova K.V., Izrailevskiy L.B., Levin A.Ya., Morozov A.M. "Influence of Accident Conditions due to Loss of Tightness by Primary Circuit on Fuel Claddings", *Proc. of the Ninth Int. Symp. on Zirconium in the Nuclear Industry*, Kobe, Japan, November 5-8, 1990 (ASTM STP-1132, 1991).
- [2] Hozer Z., Griger A., Matius L., Vasaros L., Horvath M. "Effect of Hydrogen Content on the Embrittlement of Zr Alloys", *Proc. of IAEA Technical Committee Meeting on "Fuel Behavior under Transient and LOCA Conditions"*, Halden, Norway, September 10-14, 2001.
- [3] Hozer Z., Matus L., Horvath M., Vasaros L., Griger A., Maroti L. "Ring Compression Tests with Oxidized and Hydrided Zr-1%Nb and Zircaloy-4 Cladding", Hungarian Academy of Sciences, CRIP, Budapest, Report KFKI-2002-01/G.
- [4] Vrtilkova V., Valach M., Molin L. "Oxidizing and Hydrating Properties of Zr-1%Nb Cladding Material in Comparison with Zircalloys", *Proc. of IAEA Technical Committee Meeting on "Influence of Water Chemistry on Fuel Cladding Behavior"*, Rez (Czech Republic), October 4-8, 1993.
- [5] Vrtilkova V., Novotny L., Doucha R., Vesely J. "An Approach to the Alternative LOCA Embrittlement Criterion", *Proc. of SEGFSM Topical Meeting on LOCA Fuel Issues*, Argonne National Laboratory, May 2004 (NEA/CSNI/R(2004)19).
- [6] Böhmert J. "Embrittlement of Zr-1%Nb at Room Temperature after High-Temperature Oxidation in Steam Atmosphere", *Journal, Kerntechnik* 57 No1, 1992.
- [7] Böhmert J., Dietrich M., Linek J. "Comparative Studies on High-Temperature Corrosion of Zr-1%Nb and Zircaloy-4", *Nuclear Engineering and Design*, 147 No1, 1993.
- [8] Bibilashvili Yu.K., Sokolov N.B., Salatov A.V., Andreyeva-Andriyevskaya L.N., Nechayeva O.A., Vlasov F.Yu. "RAPTA-5 Code: Modelling of Behaviour of Fuel Elements of VVER Type in Design Accidents. Verification Calculations", *Proc. of IAEA Technical Committee Meeting on "Behavior of LWR Core Materials under Accident Conditions"*, Dimitrovgrad, Russia, on 9-13 October 1995. IAEA-TECDOC-921, Vienna, 1996.
- [9] Gyori Cs. et.al. "Extension of Transuranus code applicability with niobium containing models (EXTRA)". *Proc. of FISA-2003 Conference EU Research in Reactor Safety*, EC Luxembourg, November 2003.
- [10] Baker L., Just L.C. "Studies of Metal Water Reactions at High Temperatures", Technical report of ANL-6548, 1962.
- [11] Cathcart J.V. and Pawel R.E. "Zirconium Metal-Water Oxidation Kinetics: IV Reaction Rate Studies", ORNL/NUREG-17, 1977.
- [12] Mardon J.P., Garner G., Beslu P., Charquet D., Senevat J. "Update on the Development of Advanced Zirconium Alloys for PWR Fuel Rod Claddings", *Proceedings of the International Topical Meeting on Light Water Reactor Fuel Performance*, Portland, Oregon, March 2-6, 1997.
- [13] Brachet J., Pelchat J., Hamon D., Maury R., Jaques P., Mardon J. "Mechanical Behavior at Room Temperature and Metallurgical Study of Low-Tin Zry-4 and M5™ (Zr-NbO) Alloys after Oxidation at 1100°C and Quenching", *Proc. of IAEA Technical Committee Meeting on "Fuel Behavior under Transient and LOCA Conditions"*, Halden, Norway, September 10-14, 2001.
- [14] Mardon J., Frichet A., Bourhis A. "Behavior of M5™ Alloy under Normal and Accident Conditions", *Proc. of Top Fuel-2001 Meet.*, Stockholm, May 27-30, 2001.
- [15] Billone M.C., Yan Y. and Burtseva T. "Post-Quench Ductility of Zircaloy, E110, ZIRLO and M5", *Proc. of SEGFSM Topical Meeting on LOCA Fuel Issues*, Argonne National Laboratory, May 2004 (NEA/CSNI/R(2004)19).
- [16] Billone M.C., Yan Y. and Burtseva T. "Post-Quench Ductility of Advance Alloy Cladding", *2004 Nuclear Safety Research Conference*, Washington DC, October 2004.

- [17] Mardon J.P., Waeckel N. "Behavior of M5TM Alloy under LOCA Conditions", *Proc. of Top Fuel-2003 meetings "Nuclear Fuel for Today and Tomorrow Experience and Outlook"*, March 16-19, 2003, Wurzburg, Germany.
- [18] Waeckel N., Mardon J.P. "Recent data on M5TMAlloy under LOCA Conditions", *Proceedings of the 2003 Nuclear Safety Research Conference*, Washington DC, October 20-22, 2003, NUREG/CP-0185, 2004.
- [19] Nikulina A.V., Andreeva-Andrievskaya L.N., Shishov V.N., Pimenov Yu.V. "Influence of Chemical Composition of Nb Containing Zr Alloy Cladding Tubes on Embrittlement under Conditions Simulating Design Basis LOCA", *Fourteenth International Symposium on Zirconium in the Nuclear Industry*, ASTM STP.

